

MCPIP-1-Mediated Immunosuppression of Neutrophils Exacerbates Acute Bacterial Peritonitis and Liver Injury

Jian Lin^{a,b} Zhanjun Lu^c Gengfeng Li^a Cui Zhang^a Huiying Lu^a Sheng Gao^d
Ruixin Zhu^d Hailiang Huang^e Konrad Aden^f Jianhua Wang^g Yingzi Cong^h
Huili Wuⁱ Zhanju Liu^a

^aDepartment of Gastroenterology, Shanghai Tenth People's Hospital of Tongji University School of Medicine, Shanghai, China; ^bDepartment of Gastroenterology, Affiliated Hospital of Putian University, Putian, China; ^cDepartment of Gastroenterology, Shanghai General Hospital, Shanghai Jiao Tong University School of Medicine, Shanghai, China; ^dDepartment of Bioinformatics, School of Life Sciences and Technology, Tongji University, Shanghai, China; ^eAnalytic and Translational Genetics Unit, Massachusetts General Hospital, Boston, MA, USA; ^fDepartment of Internal Medicine I, Institute of Clinical Molecular Biology, Christian-Albrechts-University, University Hospital Schleswig-Holstein, Campus Kiel, Kiel, Germany; ^gStorr Liver Unit, Westmead Millennium Institute, Westmead Hospital, University of Sydney, Sydney, NSW, Australia; ^hDepartment of Microbiology and Immunology, University of Texas Medical Branch, Galveston, TX, USA; ⁱDepartment of Gastroenterology, Zhengzhou Central Hospital Affiliated to Zhengzhou University, Zhengzhou, China

Keywords

MCPIP-1 · Neutrophils · Acute bacterial peritonitis · Liver injury · Bacterial infection

Abstract

Monocyte chemoattractant protein-1-induced protein-1 (MCPIP-1) is highly expressed in activated immune cells and negatively regulates immune responses, while the mechanisms underlying the immunoregulation of neutrophils in acute bacterial infection and liver injury remain elusive. Here, we examined the role of MCPIP-1 in regulating neutrophil functions during acute bacterial peritonitis and liver injury. Mice with myeloid cell-specific overexpression (*Mcpip*^{Mye-tg}) or knockout (*Mcpip*^{ΔMye}) of MCPIP-1 were generated. We found that reactive oxygen species and myeloperoxi-

dase production, formation of neutrophil extracellular traps, and migratory capacity were deficient in *Mcpip*^{Mye-tg} neutrophils but enhanced in *Mcpip*^{ΔMye} neutrophils. The recruitment of neutrophils and pathogen clearance were markedly suppressed in *Mcpip*^{Mye-tg} mice following intraperitoneal infection with *Salmonella typhimurium* while intensified in *Mcpip*^{ΔMye} mice. Severe acute *S. typhimurium*-infected peritonitis and liver injury occurred in *Mcpip*^{Mye-tg} mice but were alleviated in *Mcpip*^{ΔMye} mice. RNA sequencing, RNA-binding protein immunoprecipitation and qPCR analysis revealed that MCPIP-1 downregulated the protective functions of neutrophils via degrading the mRNA of cold inducible RNA-binding protein. Consistently, MCPIP-1 was highly expressed

Jian Lin and Zhanjun Lu share the first authorship.

in neutrophils of patients with acute infectious diseases, especially in those with liver injury. Collectively, we uncover that MCPIP-1 negatively regulates the antibacterial capacities of neutrophils, leading to exacerbating severe acute bacterial peritonitis and liver injury. It may serve as a candidate target for maintaining neutrophil homeostasis to control acute infectious diseases.

© 2022 The Author(s).
Published by S. Karger AG, Basel

Introduction

Acute bacterial peritonitis (ABP) is one of the most severe diseases in critical care medicine, which could be secondary to the acute abdominal diseases, such as acute severe pancreatitis, intestinal perforation, and acute appendicitis. With the characteristic of a rapid onset, the incidence of dangerous situations, high mortality, and poor prognosis, ABP is a significant economic burden for health systems worldwide [1–3]. In the severe stage of ABP, such as sepsis or bacteremia, the risk of death could be increased as a result of intestinal barrier damage, dysregulated immune regulation, and multiple organ injuries. The liver could be the target organ being attacked by pathogens via intestinal hepatic circulation or systemic blood circulation in the progress of sepsis [4, 5]. As one of the essential organs that associate with pathogen clearance, it has been confirmed that over 60% of invading pathogens would be captured by the liver in 10 min in an intravenous bacterial injection model [6]. Hepatic endothelial cells, stellate cells, Kupffer cells, and neutrophils in hepatic sinuses play an important role in immune surveillance and elimination of pathogenic microorganisms.

Neutrophils are the most abundant immune cells in the circulation and an essential effector of innate immune response and immune homeostasis [7]. In the context of the invasion and attack of exogenous pathogens, neutrophils are rapidly recruited into the sites of infection via chemotactic signals, e.g., CXCL8 (IL-8) and CXCL-1/2 [8], and eliminate pathogens through the phagocytosis and release of reactive oxygen species (ROS) and antimicrobial peptides [9, 10]. Importantly, in response to various inflammatory stimuli, neutrophils play important roles in host defense through the formation of neutrophil extracellular traps (NETs) and the release of proteases [11]. It has been suggested that ABP-related organ injury would occur due to insufficient neutrophil mobilization [12]. Collectively, these data indicate that neutrophils play a critical role in defense against

pathogen invasion. However, the mechanisms underlying the delicate immunoregulation of neutrophils are still not fully defined.

Monocyte chemotactic protein-1-induced protein-1 (MCPIP-1), namely, Regnase-1, is encoded by the ZC3H12A gene [13], which represents a zinc finger protein and is expressed at a low level in most cells but rapidly increased by a variety of inflammatory stimuli including MCP-1, Toll-like receptor ligands, IL-1 β , and TNF- α [14]. MCPIP-1 has been found to function as a negative regulator in macrophages and acts to remove ubiquitin moieties attached to proteins (e.g., TRAF2, TRAF3, and TRAF6) and suppress c-Jun N-terminal kinase and NF- κ B signaling pathways subsequently [15]. Accumulating lines of evidence have demonstrated that MCPIP-1 acts as an endonuclease to degrade the mRNAs of some inflammatory cytokines (e.g., IL-1 β , IL-12, IL-6, and IL-2) [14, 16], and most importantly, it degrades the mRNA of itself as a negative feedback to the synthesis of MCPIP-1 [16]. Meanwhile, MCPIP-1 degrades and restrains the biosynthesis of several microRNAs such as microRNA-135b, -21, -155, -146a, -143, and -145 [17]. Moreover, MCPIP-1 also negatively modulates T-cell activation and some tumor cell proliferation and differentiation (e.g., breast cancer, clear cell renal cell carcinoma) [18, 19]. In agreement with the results above, MCPIP-1 has been reported to alleviate the inflammation responses in the noninfectious models, such as LPS-induced sepsis, via inhibiting the activity of macrophages or B cells [20, 21], indicating that MCPIP-1 plays an important role in balancing dysregulated activation of immune cells delicately. Our recent study has demonstrated that MCPIP-1 is highly expressed in peripheral neutrophils and markedly increased under chronic inflammatory conditions, particularly in inflammatory bowel diseases, and downregulates the activity of neutrophils [22]. However, the role of MCPIP in modulating myeloid cell (i.e., neutrophil, monocyte, macrophage) functions, especially neutrophils that constitute the first defense line to exogenous pathogens [23], in ABP, and in secondary organ injury (e.g., liver injury) is still poorly understood.

In this study, we aimed to clarify the roles of MCPIP-1 in modulating myeloid cells, particularly neutrophils, in the induction and progress of bacteria-induced acute peritonitis and liver injury and revealed that MCPIP-1 negatively regulated the antibacterial capacities of neutrophils, leading to exacerbating severe ABP and liver injury.

Materials and Methods

Human Samples

All patients were recruited from the Departments of Gastroenterology, Respiratory, and Critical Care Medicine and the Abdominal Pain Center, Shanghai Tenth People's Hospital of Tongji University (Shanghai, China), from October 2019 to May 2021. EDTA-anticoagulated blood samples (15–20 mL) were obtained from patients with active Crohn's disease with peritoneal exudation (CDE, $n = 10$), patients with acute pancreatitis ($n = 10$), patients with acute suppurative appendicitis ($n = 10$), patients with community-acquired bacterial pneumonia (CABP, $n = 10$), and healthy controls ($n = 10$) after overnight fasting. The clinical characteristics of these patients were shown in online supplementary Table 1 (see www.karger.com/doi/10.1159/000526784 for all online suppl. material). The diagnoses for acute abdominal inflammatory diseases were based on clinical characteristics, radiological and endoscopic examination, and histological findings, while the diagnosis for CABP was based on clinical manifestations, sputum bacterial culture, and chest CT scanning. Primary hepatitis and other diseases of the biliary system were excluded in acute pancreatitis, which may interfere with the results. All patients were in general wards before receiving any antimicrobials when blood samples were collected. This study was approved by the Institutional Review Board for Clinical Research of Shanghai Tenth People's Hospital of Tongji University (Approval No. SHSY-IEC-40.0/19-37/01).

Mice

Mice with targeted overexpression of MCPIP-1 in myeloid cells (*Mcpip*^{Mye-tg} mice), the MCPIP-1-LoxP mice (*Mcpip*^{fl/fl} mice), and LysM-Cre mice (all on a C57BL/6J background) were presented kindly by Drs. Jianli Niu and Pappachen Kolattukudy from the Burnett School of Biomedical Science, College of Medicine, University of Central Florida (Orlando, USA). *Mcpip*^{Mye-tg} mice and myeloid cell-specific MCPIP knockout (*Mcpip*^{ΔMye}) mice were generated using the protocol as described previously [24]. To generate *Mcpip*^{Mye-tg} mice, murine LysM promoter (5532 bp) from mouse chromosome 10 position 116724852 to 116719328 was fused to murine MCPIP-FLAG in a pBluescript vector. A 7,332-bp NotI-XhoI fragment containing the LysM promoter fused to MCPIP was purified by gel electrophoresis and microinjected into fertilized C57BL/6J mouse ova at the MD Anderson Cancer Center (Houston, TX, USA). Genotyping was carried out using PCR with specific primers in the LysM promoter region and the transgenic coding region. The transgene-containing founders were bred with C57BL/6J mice to generate F1 transgenic mice, and wild-type (WT) C57BL/6J mice were used as control mice when *Mcpip*^{Mye-tg} mice were used for experiments. The *Mcpip*^{ΔMye} mice were generated by crossing *Mcpip*^{fl/fl} mice and LysM-Cre mice. Expression of MCPIP-1 in neutrophils was identified in online Supplementary Figure 1. WT C57BL/6J mice were bred at the Animal Experimental Center of Tongji University School of Medicine, and all mice were raised under SPF conditions with filtered air in microisolator cages and fed autoclaved food and water at our animal facility. All male mice with 18–20 g of body weight and aged 6–8 weeks were used for experiments. Animal studies were reviewed and approved by the Institutional Animal Care and Use Committee of the Tongji University (Approval No. SHDSYY-2018-1966).

Reagents and mAbs

Cell culture reagents including RPMI-1640 medium, fetal bovine serum (FBS), streptomycin/penicillin, 2-mercaptoethanol, and phosphate-buffered saline (PBS) were all purchased from HyClone (Logan, UT, USA). Phorbol 12-myristate 13-acetate (PMA), ionomycin, collagenase IV, and deoxyribonuclease I (DNase I) were all purchased from Sigma-Aldrich (St. Louis, MO, USA). The Amplex Red Hydrogen Peroxide/Peroxidase Assay Kit for measuring the levels of ROS or MPO was purchased from Thermo Fisher Scientific (Carlsbad, CA, USA). The Phagocytosis Assay Kit (Green *E. coli*) was purchased from Abcam (Cambridge, UK). The mAbs used for flow cytometry in this study were purchased from BioLegend (San Diego, CA, USA). All primers were synthesized and purchased from ShengGong BioTeck (Shanghai, China).

Isolation of Neutrophils

Neutrophils were isolated from peripheral blood following the protocol as described previously within 4–6 h after the inclusion of patients [25]. Peripheral blood was collected in EDTA-anticoagulated tubes and slowly laid on the surface of Ficoll (GE Healthcare, Piscataway, NJ, USA), followed by gradient centrifugation at 2,000 rpm at 20°C. The lowest layer was collected, and neutrophils were obtained after incubating with red blood cell lysis buffer (BD Biosciences, San Diego, CA, USA). The isolation of neutrophils from the bone marrow of mice ($n = 6$ in each group) was performed using a murine neutrophil isolation kit according to the manufacturer's instructions (Miltenyi Biotec, Bergisch Gladbach, Germany). The neutrophils from the bone marrow for in vitro experiments were isolated from the mice under naïve conditions.

Cell Culture

The HL-60 cell line was purchased from the Chinese Academy of Science (Shanghai, China). The HL-60 cell line was cultured in IMDM medium supplemented with 20% FBS, penicillin (100 U/mL), and streptomycin (100 μg/mL) at 37°C with 5% CO₂ and differentiated into granulocyte-like cells (dHL-60) by addition of 1.3% DMSO (Gibco, Carlsbad, CA, USA) after 96 h. The percentage of CD66b⁺ cells was analyzed by flow cytometry to testify the efficiency of the differentiation. dHL-60 cells were stimulated with Pam3CSK4 (1 μg/mL; APEX BIO, Houston, TX, USA), FSL (100 ng/mL; Abcam), LPS (100 ng/mL; Sigma-Aldrich), flagellin (100 ng/mL; InvivoGen, Toulouse, France), and PGN (1 μg/mL; Sigma-Aldrich), respectively, and collected 3 h after stimulation.

Adenovirus Transduction

A recombinant adenovirus over-expressing MCPIP-1 (AV-MCPIP-1, target sequencing: TCCTTG TAGTCCATACCCTCACTGGGGTGCTGGGACTTG), AV over-expressing D141N mutant (AV-D141N, target sequencing: TCCTTG TAGTCATACCCTCACTGGGGTGCTGGGACTTG TAG), and AV over-expressing cold inducible RNA-binding protein (CIRBP) shRNA (AV-sh-CIRBP, target sequencing: CTC AAAGTACGGA-CAGAT) were constructed in GeneChem (Shanghai, China). The over-expressing MCPIP-1 or D141N mutant sequence was synthesized using CMV-MCS-3FLAG-SV40-EGFP vector, and the CIRBP shRNA was synthesized using hU6-MCS-Ubiquitin-EGFP-IRES vector. The HL-60 cell suspensions (2 mL, 10⁵/mL) were seeded in a 12-well plate, and they were transduced with AV-MCPIP-1, AV-D141N, AV-sh-CIRBP, and negative control AV-NC, respectively, at 37°C with 5% CO₂ for 16 h. Then the HL-60

cells were collected. After centrifugation and resuspension with IMDM, the HL-60 cell suspensions were seeded in a new 12-well plate at 37°C with 5% CO₂ for 72 h. After transfection, the expression of the target gene in transfected HL-60 cells was measured by quantitative real-time PCR (qRT-PCR) to determine the efficiency of transfection. The transfected HL-60 cells were suspended with IMDM and moved into a T-25 bottle for further experiments. All of the vectors were found not to affect the efficiency of dHL-60 cell differentiation (online Suppl. Fig. 2).

Establishment of Salmonella typhimurium-Induced Acute Peritonitis

The *Salmonella typhimurium* strain (ATCC14028) was provided kindly by Dr. Guangxun Meng from the Shanghai Institute of Pasteur, Chinese Academy of Sciences (Shanghai, China). The bacteria were stored and generated following the protocol as described previously [26]. The mice ($n = 6$ in each group) were infected by *S. typhimurium* via intraperitoneally injecting 100 μ L of suspension of *S. typhimurium* (5×10^6 CFU/mL). Control mice ($n = 6$ in each group) were injected intraperitoneally 100 μ L of LB liquid medium. At 24 h after peritonitis induction, we intraperitoneally injected 4% chloral hydrate with 0.1 mL/10 g in these mice and observed the disappearance of corneal reflex which was considered in deep anesthesia. Peripheral blood was immediately drawn from the vein cluster behind the eyeball of the mice. Mice were injected intraperitoneally with 10 mL of sterile PBS and then extracted after gently shaking for 30 s to take the peritoneal lavage in 10 min after blood collection. The analysis of the samples of peripheral blood and peritoneal lavage was performed by Servicebio Corp (Wuhan, China). To measure the load of *S. typhimurium*, we sacrificed the mice immediately through carbon dioxide inhalation under deep anesthesia after peritonitis induction. Then, we removed and cut the liver tissues into pieces after being weighed, followed by being diluted with LB liquid medium (3 mL). The mixture of liver tissues and LB liquid medium was mixed and stirred fully after 3–5 times. Then 1 mL of tissue suspension was extracted and homogenized thoroughly. All samples including peripheral blood, peritoneal lavage, and suspension of liver tissues were then seeded into LB plates (BD Biosciences) by a 10-fold serial concentration gradient and incubated at 37°C with 5% CO₂ for 18 h. The minimum dilution in which the colony of bacteria could be observed was set as the baseline number. The load of *S. typhimurium* was shown as the logarithm of the colony number and the baseline number.

Analysis of Neutrophil Bactericidal Function

Neutrophils (5×10^5 cells/mL) isolated from mice ($n = 5$ in each group) were added into a 24-well plate. Suspension of *S. typhimurium* (10 μ L, 5×10^6 CFU/mL) was added to the wells and incubated for 3 h at 37°C. Then, the supernatant in each well was added into LB plates (BD Biosciences) by a 10-fold serial concentration gradient and incubated at 37°C with 5% CO₂ for 18 h. The minimum dilution in which the colony of bacteria could be observed was set as the baseline number. The load of *S. typhimurium* was shown as the logarithm of the colony number and the baseline number.

Immunofluorescence Staining

Immunofluorescence staining was performed using our protocol as described previously [22]. Briefly, liver tissues were freshly harvested from the sacrificed mice, and cryostat-cut sections were

then prepared. These sections were first stained with either anti-F4/80 or anti-MPO mAb (both from Abcam) and incubated continuously with Alexa Fluor[®] 594-conjugated donkey anti-rabbit IgG (Abcam) for 1 h at room temperature. Finally, the sections were stained with Hoechst 33342 (MCE; Monmouth Junction, NJ, USA), mounted with a coverslip, and viewed by immunofluorescence microscopy.

Preparation of Immune Cells in Liver Tissues

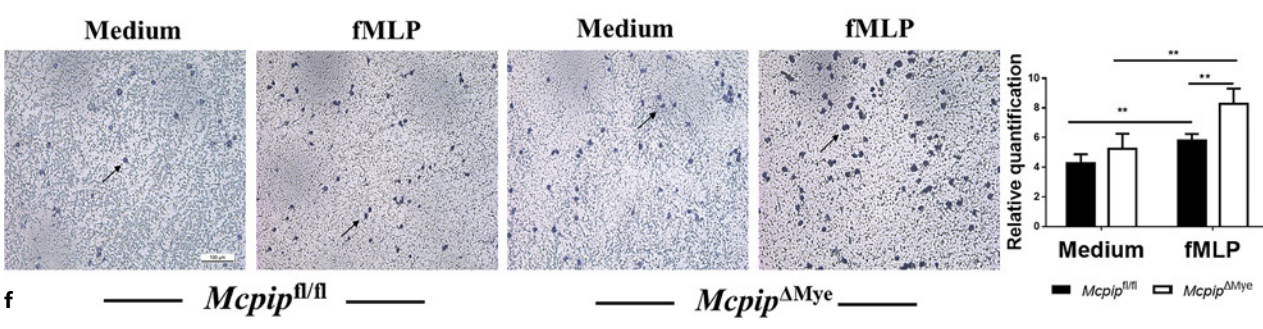
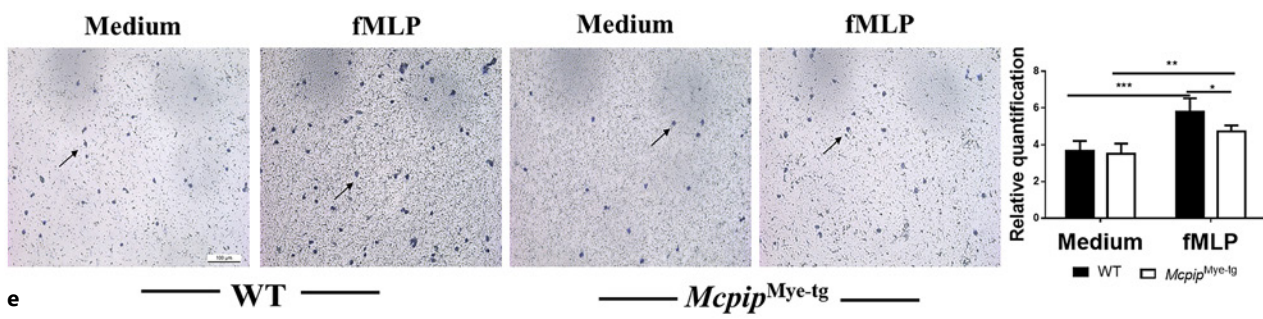
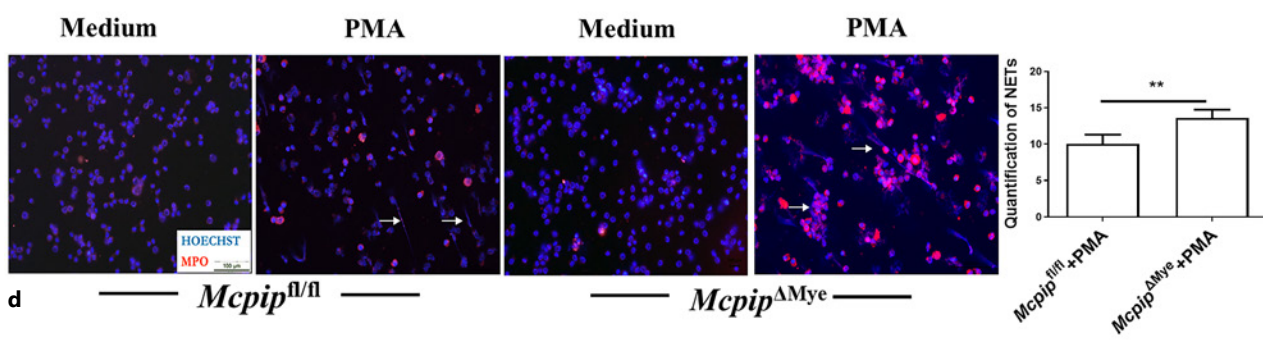
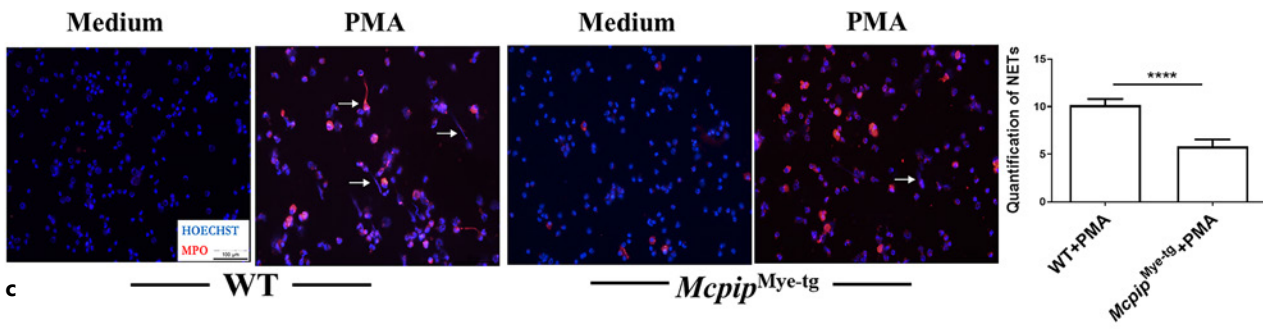
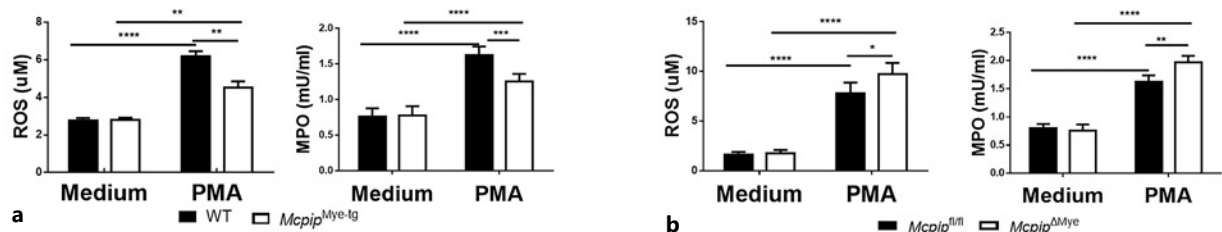
Under deep anesthesia, a catheter (diameter 0.45 mm) was carefully inserted into the portal vein and fixed firmly, and the inferior vena cava was cut for blood outflow. The liver was perfused with PBS until the liver turned pale and then removed carefully into a sterilized bottle. The liver was chopped into small pieces and incubated for digestion in 9.8 mL PBS supplemented with 0.005% collagenase IV, 0.02% FBS, and 0.001% DNase I for 20 min at 37°C. After being filtered through a 100- μ m nylon cell strainer and centrifuged, the cells were subsequently resuspended in 4 mL of 40% Percoll in PBS, gently overlaid onto 2 mL of 75% Percoll, and centrifuged at 2,000 rpm for 20 min. The cells were collected from the interface and washed with PBS. To analyze the composition of the cells, all cells were resuspended by FACS buffer and then stained with suitable mAbs for 30 min at 4°C after counting. For intracellular cytokine staining, the immune cells were stimulated with PMA (500 ng/mL) and ionomycin (750 ng/mL) in the presence of brefeldin A (1 μ g/mL, BioLegend) for the last 4 h of incubation at 37°C. Data were then acquired on BD FACS Canto II (BD Biosciences).

Western Blotting Analysis

Cell depositions were lysed by radioimmunoprecipitation assay and phenylmethylsulfonyl fluoride (1 mM). After centrifugation, the total protein was obtained. Samples were then resolved on sodium dodecyl sulfate-polyacrylamide gel electrophoresis (Epi-Zyme, Shanghai, China) by standard procedure. Western blotting was performed as described previously [27]. Immunoblotting was performed with human primary antibodies to MCP-1 (Santa Cruz), p65 (1:100, Servicebio), and β -actin (Abcam), respectively. The Odyssey Infrared Imaging System and Image Studio (LI-COR Biosciences, Lincoln, NE, USA) were used for signal detection. Image J (National Institutes of Health; Bethesda, MD, USA) was used for quantification.

Quantitative Real-Time PCR

Total RNA from neutrophils and liver tissues was extracted with TRIzol (Life Technologies, Carlsbad, CA, USA). The concentration and purity of RNA were determined by a NanoVue spectrophotometer (GE Healthcare), and the quality and quantity of RNA of each sample were assessed through NanoDrop 2000 (Thermo Fisher Scientific) with an A260/A280 ratio of >1.8 and <20.0 for samples. We synthesized cDNA from 400 ng of RNA using an all-in-one reverse transcription reagent kit (abm; Richmond, BC, Canada). PCR was performed using a SYBR Green PCR Kit (Takara, Dalian, China) in the ABI prism 7900 HT sequence detector (Applied Biosystems, Foster City, CA, USA). The qRT-PCR reaction conditions were as follows: 95°C for 1 min, 95°C for 15 s, and 60°C for 30 s repeated for 40 cycles as described previously [28]. All primers were synthesized by Sangon BioTech (Shanghai, China), and GAPDH was used as a housekeeping gene. qRT-PCR analysis was calculated with the $2^{-\Delta\Delta C_t}$ method.



(For legend see next page.)

Analysis of the NET Formation

Murine bone marrow-derived neutrophils were isolated and stimulated with PMA (100 ng/mL) at 37°C with 5% CO₂ for 3 h. They (1×10^5) were seeded on the poly-L-lysine-coated glass slide, fixed with 4% paraformaldehyde, and then incubated with the anti-MPO antibody (Abcam) at 4°C overnight. The slides were incubated with Alexa Fluor[®] 594-conjugated donkey anti-rabbit IgG (Abcam) for 1 h at room temperature. After 3 washes, the sections were stained with Hoechst 33342 (MCE), and NETs were visualized on immunofluorescence microscopy (DFC7000T; Leica, Wetzlar, Germany).

Neutrophil suspensions (270 μ L, at a concentration 1×10^5 /mL) were loaded in a 96-well plate and then stimulated with PMA (100 ng/mL) together with or without DNase (0.1 mg/mL) for 45 min at 37°C with 5% CO₂. One sample of cell suspensions was incubated with TX-100 (the final concentration of 0.3%) in each group to measure total DNA. All wells were treated with SYTOX Green (30 μ L, the final concentration of 0.1 mg/mL, Invitrogen, Carlsbad, CA, USA) and incubated for 15 min at room temperature. The fluorescence value (FV) of each well was measured in a BioTek-Synergy-2 fluorometric plate reader (BioTek, Oxford, UK) with a filter setting of 485-nm excitation and 530-nm emission. The mean was calculated from 3 wells for each group. The quantification of NETs was performed as follows: the FVs of the neutrophils stimulated with PMA without DNase subtracted the FVs of the neutrophils stimulated with PMA in the presence of DNase in the same group, and the results were then divided by the FVs of the neutrophils incubated with TX-100 in the same group. Moreover, dHL-60 cells were also stimulated in vitro with ionomycin (4 μ g/mL) to release NETs, and the rest procedures were performed using the same procedure as described previously [29].

Transwell Assay

Transwell migration assay was performed to detect the migratory capacity of neutrophils using a method as described previously [30]. Briefly, neutrophils (1×10^5) were loaded into the up-

Fig. 1. MCPIP-1 downregulates the production of ROS and MPO and the formation of NETs and suppresses the migratory capacity of neutrophils. Neutrophils (1×10^6) were isolated from the bone marrow of *Mcpip*^{Mye-tg} ($n = 6$), WT ($n = 6$), *Mcpip* ^{Δ Mye} ($n = 6$), and *Mcpip*^{fl/fl} mice ($n = 6$) and stimulated in vitro with or without PMA (100 ng/mL) for 3 h. **a, b** Expression of ROS and MPO was determined by the Amplex Red Hydrogen Peroxide/Peroxidase Assay Kit. **c, d** Representative immunofluorescent images for detecting NETs (blue, Hoechst 33342; red, MPO. Scale bars, 100 μ m). The quantification of NETs was calculated according to the formula as described in the Methods section. **e, f** Neutrophils (5×10^6) were isolated from the bone marrow of *Mcpip*^{Mye-tg} ($n = 6$), WT ($n = 6$), *Mcpip* ^{Δ Mye} ($n = 6$), and *Mcpip*^{fl/fl} mice ($n = 6$). The chemoattraction of neutrophils was induced by fMLP (50 nM) for 3 h using a 5- μ m Transwell plate. Representative images of lower chambers of Transwell plates were shown. Scale bars, 100 μ m. The black arrows indicate neutrophils stained by crystal violet. The histograms represented the relative quantification of the migratory capacity of neutrophils by measuring the OD values of each well as described above. * $p < 0.05$; ** $p < 0.01$; *** $p < 0.001$.

per chamber of a 5- μ m Transwell plate (for dHL-60 cells or murine neutrophils), and 100 μ L of fMLP (50 nM, Sigma-Aldrich) was added into the lower chamber. Neutrophils were extracted after 3 h of culture, and each plate was fixed by 4% paraformaldehyde and stained and blotted by 0.1% crystal violet carefully after 2 washes by PBS. The plates were viewed under the inverted microscopy (DMI1, Leica). To quantify the capacity of Transwell, 33% acetic acid was added to each well to decolorize crystal violet for 30 min. The optical density (OD) of each well was detected at 570 nm. The relative quantification was calculated as the OD of acetic acid with decolorization of crystal violet dividing the OD of acetic acid alone.

RNA Sequencing

RNA-seq analysis of neutrophils sorted from *Mcpip*^{Mye-tg} and WT mice was performed using the following method. Briefly, the RNA libraries (GeneChem; Shanghai, China) were first prepared from RNA preparations with the KAPA Stranded RNA-Seq Library Prep Kit (Roche biology; Shanghai, China). They were sequenced on the HiSeq 4000 platform (Illumina, San Diego, CA, USA), and paired-end 150-base pair-long reads were generated. Clean reads were obtained from raw reads by removing adaptors and low-quality bases with Trimmomatic (version 0.36). Clean reads were mapped to the reference genome of *M. musculus* GRCm38 and used to calculate gene expression with STAR (version 2.5.3a). Genes with low-dispersion were removed with HTS-Filter R package (version 1.30.1). Differentially expressed genes were analyzed by DESeq2 package (version 1.30.0), with an adjusted p value < 0.05 .

Correlation Analysis of Differentially Expressed Genes

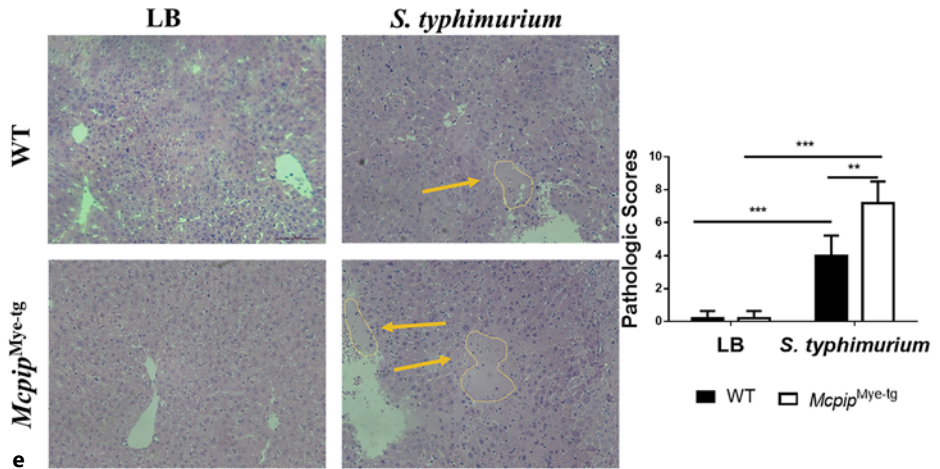
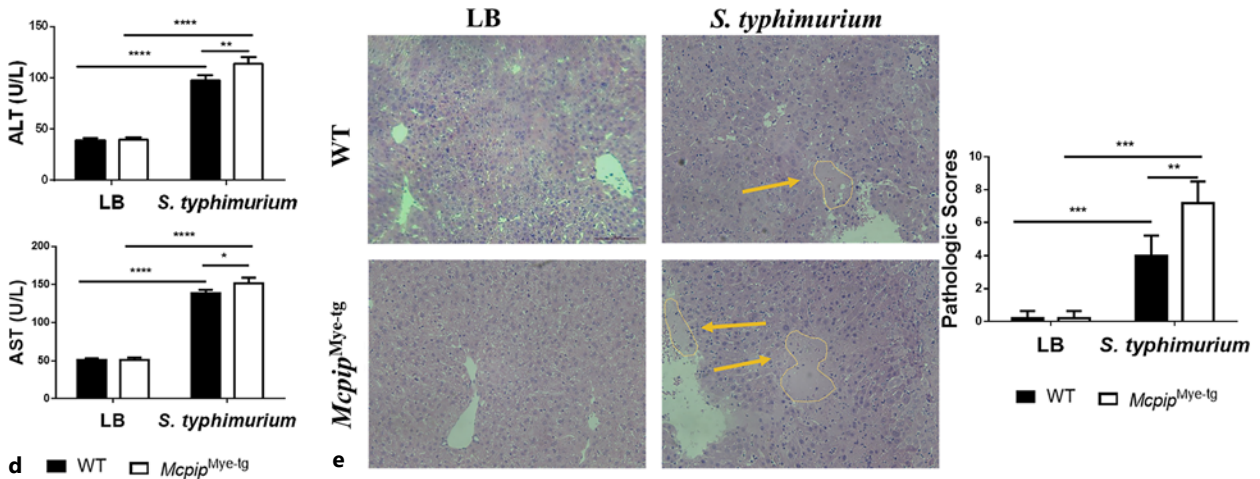
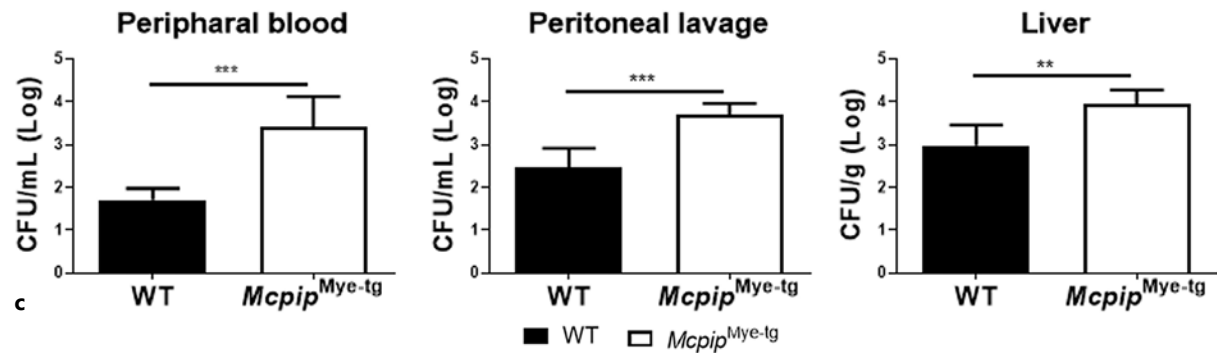
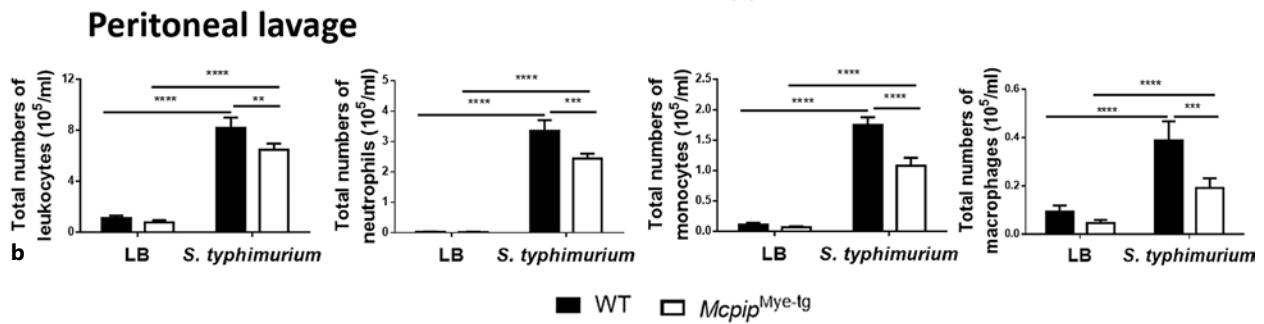
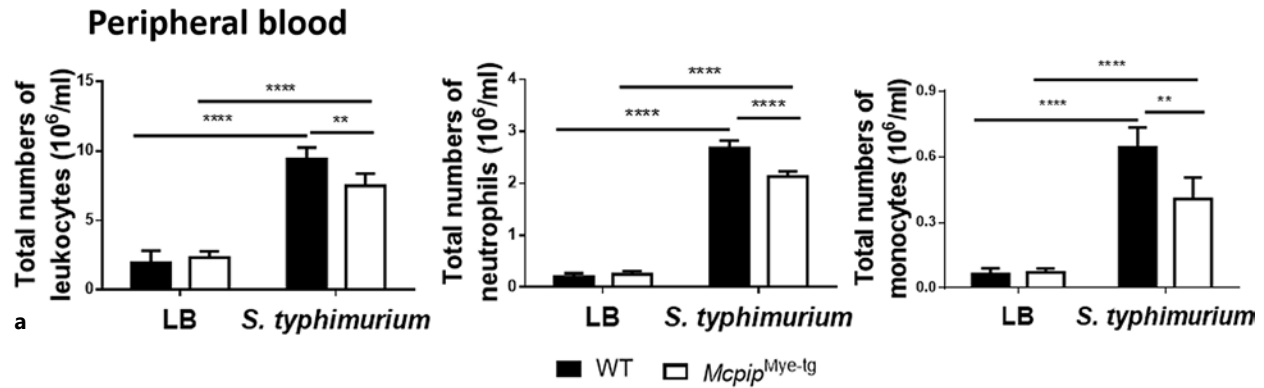
Correlation analysis of differentially expressed genes was performed with the “Spearman” method based on gene expression profile. The relations between genes with an absolute value of correlation coefficient more than 0.8 were retained. Network construction and visualization were carried out by Cytoscape (version: 3.8.0).

RNA-Binding Protein Immunoprecipitation Assay

RNA-binding protein immunoprecipitation (RIP) assay was performed using a method as described previously [31]. Briefly, cell depositions were lysed by radioimmunoprecipitation assay and phenylmethylsulfonyl fluoride (at the final concentration of 1 mM). The total protein-RNA complex was extracted by the RIP Immunoprecipitation Kit according to the manufacturer's instructions (Millipore, Danvers, MA, USA). For departing the protein and the RNA attaching to protein, the total protein-RNA complex was incubated by Proteinase K Buffer and RIP Wash Buffer. The RNA was extracted with TRIzol, and the RIP analysis was performed by GeneChem.

Statistical Analysis

All data were expressed as mean \pm SEM and analyzed using Prism V.60.0 software (GraphPad Software, San Diego, CA, USA) and SPSS V.20.0.0 (SPSSs, Chicago, IL, USA). Statistical comparisons were performed using an unpaired two-tailed Student's t test for 2 groups and one-way ANOVA for more than 2 groups. p value < 0.05 was considered to be statistically significant.



Results

MCPIP-1 Downregulates the Production of ROS and MPO and the Formation of NETs in Neutrophils

Since MCPIP-1 has been reported to inhibit the polarization of macrophages [21] and promote the apoptosis of neutrophils [32], the underlying molecular mechanisms whereby MCPIP-1 regulates the immune functions of neutrophils remain unknown. To this end, we isolated neutrophils from the bone marrow of *Mcpip*^{Mye-tg} and WT mice and assessed the production of ROS and MPO by neutrophils under spontaneous or PMA-stimulated conditions. Figure 1a shows that the ROS and MPO production was relatively low in both *Mcpip*^{Mye-tg} and WT neutrophils at a steady state, with no statistical difference. Upon PMA stimulation, MPO and ROS were significantly increased in both groups of neutrophils. Interestingly, the levels of MPO and ROS were statistically lower in PMA-treated *Mcpip*^{Mye-tg} neutrophils compared with WT controls (Fig. 1a). We further determined the formation of NETs in neutrophils under the conditions of MCPIP-1 overexpression. Neutrophils isolated from the bone marrow of *Mcpip*^{Mye-tg} and WT mice were stimulated with PMA in vitro for 3 h and then stained with Hoechst 33342, a dye that stains both intracellular and extracellular nucleic acid, and anti-MPO, a bactericidal component of NETs. Interestingly, we found that the formation of NETs was hardly observed in neutrophils of *Mcpip*^{Mye-tg} mice and that the quantification of NETs was significantly lower in *Mcpip*^{Mye-tg} neutrophils than in WT controls (Fig. 1c). However, there was no difference in the production of S1000A8 and S1000A9 between two groups of neutrophils when stimulated with LPS in vitro (online Suppl. Fig. 3a). We also tested the efficiency

Fig. 2. MCPIP-1 overexpression in myeloid cells impairs myeloid cell recruitment and pathogen elimination to deteriorate *S. typhimurium*-induced acute peritonitis and liver injury. *Mcpip*^{Mye-tg} ($n = 6$) and WT ($n = 6$) mice were challenged intraperitoneally by LB medium and *S. typhimurium* ($100 \mu\text{L}$, 5×10^6 CFU/mL), respectively, and sacrificed 24 h after bacterial infection. **a** Frequencies of leukocytes, neutrophils, and monocytes in peripheral blood from different groups. **b** Total numbers of leukocytes, neutrophils, monocytes, and macrophages in peritoneal lavage from different groups. **c** Loads of *S. typhimurium* in peripheral blood, peritoneal lavage, and the suspension of liver tissues were determined in different groups. **d** Levels of ALT and AST in sera. **e** Representative H and E staining images of the liver (original magnification, $\times 200$). The golden arrows indicate liquefactive necrosis. Scale bars, 100 μm . The changes in pathological scores from liver tissues were calculated according to the Ishak inflammation scoring system. * $p < 0.05$; ** $p < 0.01$; *** $p < 0.001$; **** $p < 0.0001$. ns, not significant; CFU, colony-forming unit.

of phagocytosis in both groups of neutrophils by the Phagocytosis Assay Kit (green *E. coli*) and observed no difference in the ability of phagocytosis (online Suppl. Fig. 3b).

We then took a complementary approach to further clarify the role of MCPIP-1 in modulating neutrophil functions and utilized neutrophils of *Mcpip* ^{Δ Mye} mice. In line with the results described above, the levels of ROS and MPO were found to be statistically higher in PMA-treated *Mcpip* ^{Δ Mye} neutrophils than in *Mcpip*^{fl/fl} littermates (Fig. 1b). Consistently, the formation of NETs was sharply increased in PMA-treated *Mcpip* ^{Δ Mye} neutrophils, and the quantification of NETs was significantly higher in PMA-treated *Mcpip* ^{Δ Mye} neutrophils than in *Mcpip*^{fl/fl} controls (Fig. 1d). Additionally, there were no differences in the production of S1000A8 and S1000A9 and phagocytosis ability between two groups (online Suppl. Fig. 3c, d).

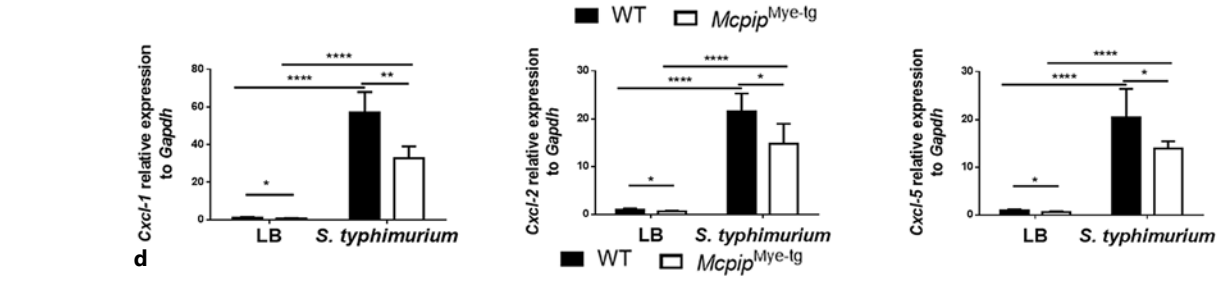
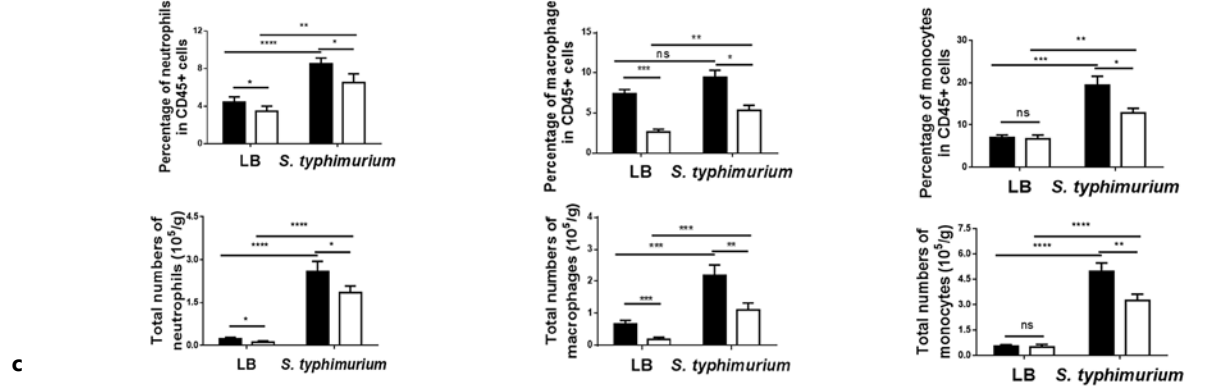
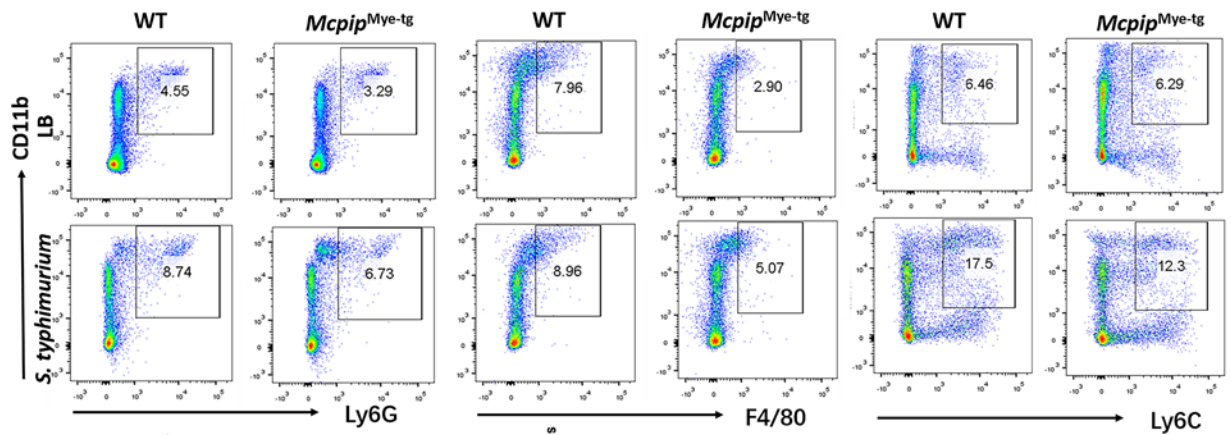
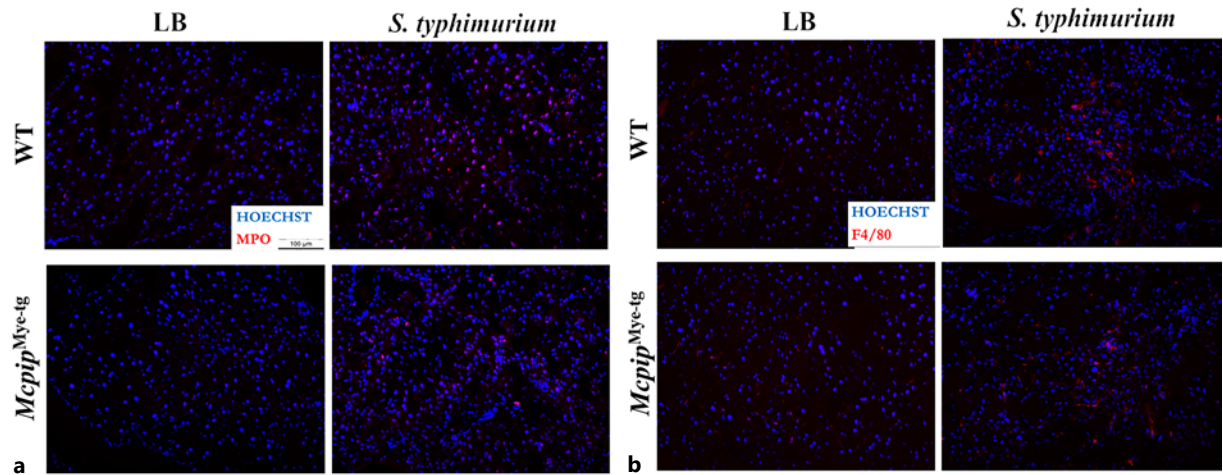
To further prove the effect of MCPIP-1 on the anti-pathogenic functions of neutrophils, we tested the bactericidal capacities of neutrophils by incubating with viable bacteria (i.e., *S. typhimurium*). We observed an increased burden of *S. typhimurium* CFU when incubated with *Mcpip*^{Mye-tg} neutrophils compared to WT controls (online Suppl. Fig. 3e). Otherwise, a sharp decrease of *S. typhimurium* load was observed when incubated with *Mcpip* ^{Δ Mye} neutrophils compared to *Mcpip*^{fl/fl} controls (online Suppl. Fig. 3e). These results indicate that MCPIP-1 could inhibit the bactericidal capacities of neutrophils in vitro. Collectively, these data confirm that MCPIP-1 inhibits the anti-pathogenic functions of neutrophils by decreasing the production of ROS and MPO and the formation of NETs, which may play a role in orchestrating the immunoregulation of neutrophils.

MCPIP-1 Suppresses the Migratory Capacity of Neutrophils

To dissect the potential roles of MCPIP-1 in the migratory capacity of neutrophils, we performed a Transwell assay to assess the migration and found that *Mcpip*^{Mye-tg} neutrophils showed a reduced migratory capacity compared to WT controls (Fig. 1e). In contrast, the migration capacity was remarkably enhanced in *Mcpip* ^{Δ Mye} neutrophils compared with *Mcpip*^{fl/fl} controls (Fig. 1f), indicating that MCPIP-1 potentially prohibits the migration of neutrophils.

*MCPIP-1 Impairs Myeloid-Cell Recruitment and Pathogen Elimination in *S. typhimurium*-Induced Peritonitis*

According to the findings as described above, MCPIP-1 could suppress the antimicrobial functions of neutrophils in vitro. Essentially, neutrophils constitute the first line of



(For legend see next page.)

host defense. We hypothesized that MCPIP-1-mediated alterations of neutrophil functions might affect the progress of anti-infectious immunity in vivo. To this end, we established an animal model of ABP by intraperitoneal infection with *S. typhimurium* [26]. *Mcpip*^{Mye-tg} and WT mice were challenged by the suspension of *S. typhimurium* via intraperitoneal injection and sacrificed at 24 h postinfection. Intraperitoneal infection with *S. typhimurium* led to a sharp influx of leukocytes into the circulation and peritoneal lavage in both WT and *Mcpip*^{Mye-tg} mice, while they were significantly reduced in *Mcpip*^{Mye-tg} mice (Fig. 2a, b). As the most abundant myeloid cells in peripheral blood and peritoneal lavage, the numbers of neutrophils increased sharply after intraperitoneal infection in both WT and *Mcpip*^{Mye-tg} mice (Fig. 2a, b). The numbers of neutrophils were lower in *Mcpip*^{Mye-tg} mice compared to WT controls under infectious conditions, while there were no differences in the percentages of neutrophils between the two groups of peripheral blood and peritoneal lavage (Fig. 2a, b; online Suppl. Fig. 4). Moreover, we observed that the numbers and percentages of monocytes in peripheral blood and peritoneal lavage and macrophages in peritoneal lavage were also significantly decreased in *Mcpip*^{Mye-tg} mice than those in WT controls after intraperitoneal infection (Fig. 2a, b; online Suppl. Fig. 4). In line with these data, we observed an increased burden of *S. typhimurium* CFU in peripheral blood, peritoneal lavage, and the liver tissues of *Mcpip*^{Mye-tg} mice compared to WT controls (Fig. 2c). Collectively, these findings indicate that the migration of myeloid cells into the circulation and peritoneal cavity increases after intraperitoneal infection with *S. typhimurium* and that MCPIP-1 could restrain such a migration of myeloid cells in vivo, thus contributing to the development of ABP.

To further confirm the findings as described above, we used the conditional knockout of *Mcpip*^{ΔMye} mice and

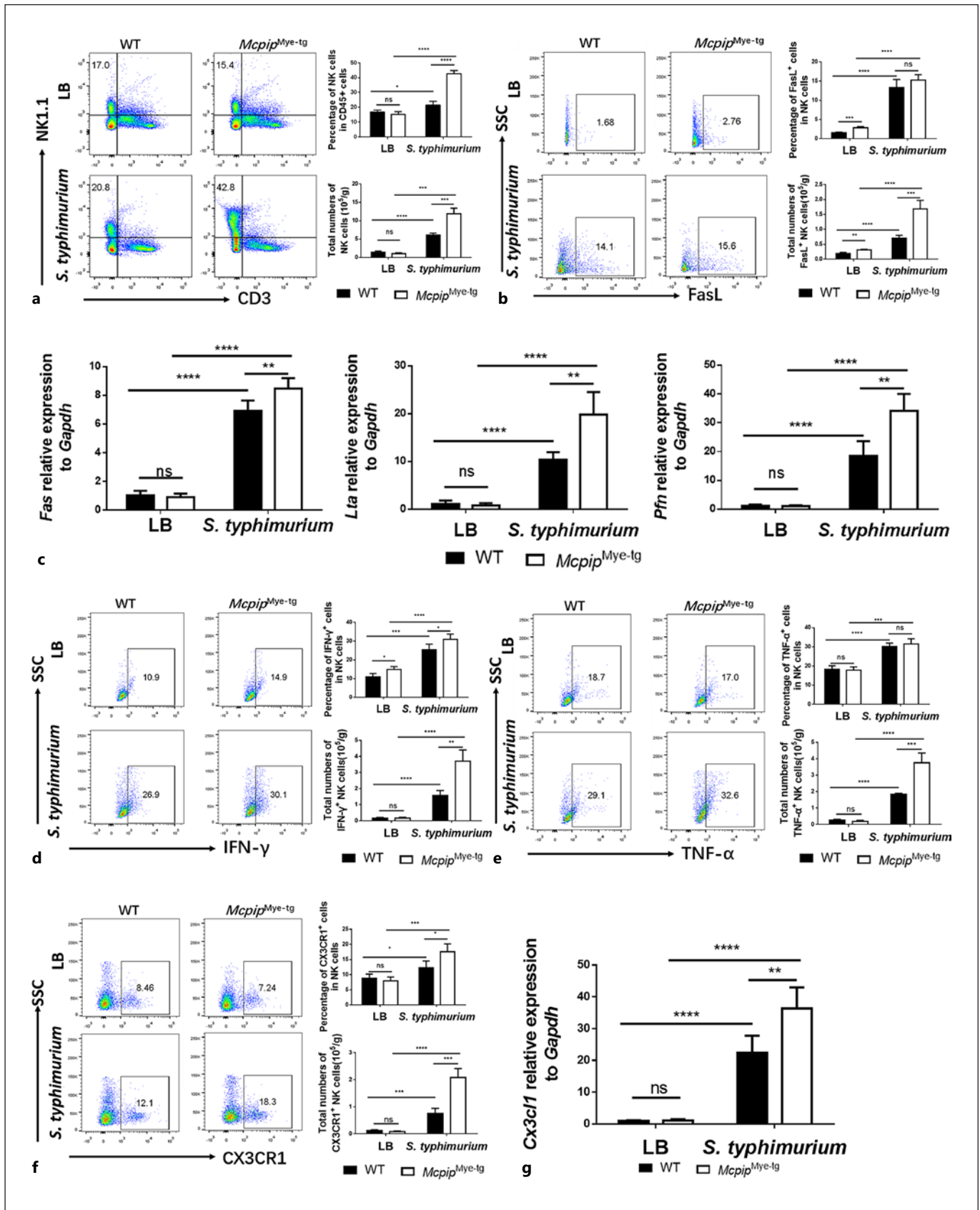
Fig. 3. MCPIP-1 suppresses the infiltration of myeloid cells into the liver and the production of chemokines in ABP. *Mcpip*^{Mye-tg} ($n = 6$) and WT ($n = 6$) mice were challenged intraperitoneally by *S. typhimurium* (100 μ L, 5×10^6 CFU/mL) and LB medium, respectively, and sacrificed 24 h after bacterial infection. **a** Representative immunofluorescent images for staining neutrophils infiltrated in the liver (red, MPO). Scale bars, 100 μ m. **b** Representative immunofluorescent images for staining macrophages infiltrated in the liver (red: F4/80). Scale bars, 100 μ m. **c** Frequencies of neutrophils, macrophages, and monocytes infiltrated in the liver were analyzed by flow cytometry (gated CD45⁺ cells). **d** Expression of *Cxcl-1*, *Cxcl-2*, and *Cxcl-5* in the liver was analyzed by qRT-PCR and normalized to GAPDH. * $p < 0.05$; ** $p < 0.01$; *** $p < 0.001$. versus the data from medium-treated group. ns, not significant.

Mcpip^{fl/fl} littermates to repeat the in vivo experiments and observed an increase of myeloid cells in both peripheral blood and peritoneal lavage but a sharp decrease of *S. typhimurium* load in peripheral blood, peritoneal lavage and the liver of *Mcpip*^{ΔMye} mice compared to those in *Mcpip*^{fl/fl} littermates (online Suppl. Fig. 5a–c, 6) 24 h after intraperitoneal infection with *S. typhimurium*. Taken together, these findings indicate that MCPIP-1 inhibits the migration of myeloid cells from the bone marrow into the circulation and then into the abdominal cavity in *S. typhimurium*-induced bacterial peritonitis and that MCPIP-1 restrains the capacity of myeloid cells to eliminate invading pathogens in *S. typhimurium*-induced peritonitis. As the most abundant myeloid cells in peripheral blood, MCPIP-1-mediated immunosuppression of neutrophils may contribute to pathogen dissemination.

MCPIP-1 Suppresses the Migration of Myeloid Cells into the Liver and Accelerates Liver Injury

Bacteria-induced peritonitis frequently causes the development of systemic inflammation and may affect the liver as a target organ [33], and bacteria may disseminate into the liver via the portal venous system [34]. To assess the tissue damage and the infiltration of bacteria and immune cells in the liver at 24 h postinfection, we measured the serum levels of alanine transaminase (ALT) and aspartate aminotransferase (AST). Figure 2d demonstrates that both ALT and AST increased after being challenged by *S. typhimurium* and that the levels of ALT and AST were significantly higher in *Mcpip*^{Mye-tg} mice than those in WT mice. Histological analysis revealed more scattered loci of the liquefactive hepatic necrosis in the liver of *Mcpip*^{Mye-tg} mice compared to WT mice (Fig. 2e).

To discern the phenotypic composition of infiltrating immune cells in the liver, we performed immunohistochemistry. MPO⁺ neutrophils and F4/80⁺ macrophages were decreased in the liver of *Mcpip*^{Mye-tg} mice compared to WT controls (Fig. 3a, b). The percentages and numbers of Ly6G⁺CD11b⁺CD45⁺ neutrophils, Ly6C⁺CD11b⁺CD45⁺ monocytes, and F4/80⁺CD11b⁺CD45⁺ macrophages were all increased in the liver of both *Mcpip*^{Mye-tg} and WT mice in response to *S. typhimurium* infection by flow cytometric analysis, whereas they were significantly decreased in *Mcpip*^{Mye-tg} mice than in WT mice (Fig. 3c). We then analyzed the expression of various chemokines including CXCL-1, CXCL-2, and CXCL-5 associated with the recruitment of neutrophils into the liver [35, 36] and found that expression of these chemokines was lower in *Mcpip*^{Mye-tg} mice than in WT mice (Fig. 3d). Intriguingly, the percentages and numbers of NK cells (CD45⁺CD3⁺NK1.1⁺ cells)



(For legend see next page.)

were observed to be significantly elevated in the liver of *Mcpip*^{Myc-tg} mice compared to those in WT mice under infectious conditions (Fig. 4a).

Accordingly, when challenged with *S. typhimurium* at 24 h postinfection, the serum levels of ALT and AST were lower in *Mcpip*^{ΔMyc} mice than those in *Mcpip*^{fl/fl} littermates (online Suppl. Fig. 5d). There were no obviously architectural changes in the liver of *Mcpip*^{ΔMyc} mice but scattered loci of the liquefactive hepatic necrosis present in *Mcpip*^{fl/fl} mice (online Suppl. Fig. 5e). Additionally, the infiltration of neutrophils, monocytes, and macrophages and expression of CXCL-1, CXCL-2, and CXCL-5 mRNA were markedly increased in the liver of *Mcpip*^{ΔMyc} mice compared with those in *Mcpip*^{fl/fl} littermates (online Suppl. Fig. 7), while the percentages and numbers of NK cells were decreased in the liver of *Mcpip*^{ΔMyc} mice compared with those in *Mcpip*^{fl/fl} littermates (online Suppl. Fig. 8a). Collectively, these results indicate that MCPIP-1 suppresses the recruitment of myeloid cells, thus contributing to the exacerbation of the liver injury.

NK Cells Are Involved in Liver Damage during Bacterial Infection

Notably, we observed that MCPIP-1 markedly inhibited the migration of myeloid cells, particularly neutrophils, into the liver tissues of *Mcpip*^{Myc-tg} mice, while large numbers of NK cells were found to be infiltrated in the liver (Fig. 4a), suggesting that NK cells might contribute to the liver injury. NK cells have been long considered as a crucial pathogenic effector in several liver diseases such as acute or chronic liver injury [37, 38], virus hepatitis [39], and liver fibrosis [40], and the underlying mechanisms whereby NK cells mediate the liver injury are mainly dependent on the Fas/FasL signaling pathway and the release of cytotoxic inflammatory mediators, such as

Fig. 4. MCPIP-1 promotes excessive NK cell infiltration into the liver in ABP. *Mcpip*^{Myc-tg} ($n = 6$) and WT ($n = 6$) mice were challenged intraperitoneally by *S. typhimurium* (100 μ L, 5×10^6 CFU/mL) and LB medium, respectively, and sacrificed at 24 h postinfection. **a** Percentages and numbers of NK cells in the liver were analyzed by flow cytometry (gated CD45⁺ cells). **b** Percentages and numbers of FasL⁺ NK cells infiltrated in the liver were analyzed by flow cytometry (gated CD45⁺ NK1.1⁺CD3⁻ cells). **c** Expression of *Fas*, *Lta*, and *Pfn* in the liver was analyzed by qRT-PCR and normalized to GAPDH. **d–f** Percentages and numbers of IFN- γ ⁺ (**d**), TNF- α ⁺ (**e**), and CX3CR1⁺ (**f**) NK cells infiltrated in the liver were analyzed by flow cytometry (gated CD45⁺ NK1.1⁺CD3⁻ cells). Lower panels show the statistical analysis of indicated cells. **g** Expression of *Cx3cl1* in the liver was analyzed by qRT-PCR and normalized to GAPDH. * $p < 0.05$; ** $p < 0.01$; *** $p < 0.001$; **** $p < 0.0001$. ns, not significant.

lymphotoxin- α , perforin, IFN- γ , and TNF- α [41, 42]. We then investigated the key effector molecules involved in NK cell-mediated liver injury. Interestingly, we found that the frequencies of FasL⁺ NK cells were significantly increased in the liver tissues of *Mcpip*^{Myc-tg} mice compared to those in WT mice at 24 h postinfection (Fig. 4b). In contrast, the frequencies of FasL⁺ NK cells were significantly decreased in the liver of *Mcpip*^{ΔMyc} mice compared to those in *Mcpip*^{fl/fl} littermates at 24 h postinfection (online Suppl. Fig. 8a, b). The levels of *Fas*, *Lta*, and *Pfn* mRNA also increased in the liver tissues of *Mcpip*^{Myc-tg} mice than those in WT mice at 24 h of *S. typhimurium* infection (Fig. 4c), while they were significantly decreased in the liver tissues of *Mcpip*^{ΔMyc} mice compared to those in *Mcpip*^{fl/fl} littermates 24 h after being challenged by *S. typhimurium* (online Suppl. Fig. 8c). Flow cytometric analysis further revealed that the frequencies of IFN- γ - and TNF- α -producing NK cells were increased in liver tissues of *Mcpip*^{Myc-tg} mice compared to those in WT mice at 24 h postinfection (Fig. 4d, e), while they were significantly lower in liver tissues of *Mcpip*^{ΔMyc} mice than those in *Mcpip*^{fl/fl} littermates at 24 h postinfection (online Suppl. Fig. 8d, e). Moreover, the CX3CL1-CX3CR1 signal pathway, crucial in recruiting NK cells [43], was increased in the liver tissues of *Mcpip*^{Myc-tg} mice than that in WT controls (Fig. 4f, g), while it was markedly reduced in the liver tissues of *Mcpip*^{ΔMyc} mice than in *Mcpip*^{fl/fl} littermates (online Suppl. Fig. 8f, g) 24 h after *S. typhimurium* infection. Collectively, our data indicate that a large number of NK cells expressing FasL, lymphotoxin- α , perforin, IFN- γ , and TNF- α infiltrated into the liver tissues due to an increased activity of the CX3CL1-CX3CR1 signal pathway, thus contributing to the induction of liver damage.

MCPIP-1 Downregulates the Activity of Neutrophils via Degrading mRNA of CIRBP

To clarify the underlying molecular mechanisms by which MCPIP-1 is associated with immunoregulation of neutrophils, we performed RNA-seq analysis of neutrophils sorted from *Mcpip*^{Myc-tg} and WT mice (online Suppl. Fig. 9) and observed hundreds of differentially expressed genes in volcano map. We selected the differentially expressed genes with extra conditions: fold change >1.5 or $<2/3$ and an adjusted p value <0.01 (Fig. 5a), and found that the expression of CIRBP, a potent positive stimulus of neutrophils in the extracellular environment [44], was decreased in *Mcpip*^{Myc-tg} neutrophils compared to WT neutrophils (Fig. 5a), which was further verified at the transcriptional levels (online Suppl. Fig. 10a). Moreover, a gene correlation network analysis (Fig. 5b) further

revealed a tight correlation between an increase of *Zc3h12a*, the gene encoding MCPIP-1, and a decrease of *Cirbp* in neutrophils. Since previous RIP-seq analysis has proven that MCPIP-1 binds the mRNA of CIRBP in HeLa cells [45], we then determined whether a decrease of CIRBP was due to an increase of RNase activity of MCPIP-1. To this end, we measured the expression of CIRBP in dHL-60 cells transfected with AV-MCPIP-1 and found that CIRBP at the transcriptional level was significantly decreased compared to controls (Fig. 5c). Additionally, we also induced overexpression of MCPIP-1 mutant D141N via transfection with AV-D141N, which is deficient in the function of RNase [14], and found that there was no effect on the expression of CIRBP at the transcriptional level (Fig. 5c). Therefore, these findings indicate that MCPIP-1 inhibits expression of CIRBP through the induction of RNase and that MCPIP-1 may bind and degrade the mRNA of CIRBP in neutrophils, leading to inhibition of the activity of neutrophils.

We then performed a RIP-qPCR analysis in dHL-60 cells to assess whether MCPIP-1 could bind the mRNA of CIRBP and observed that the fold enrichment of mRNA of CIRBP binds to MCPIP-1 was significantly increased compared to the negative controls (Fig. 5d). Therefore, these results prove that MCPIP-1 as a RNA-binding protein potentially binds the mRNA of CIRBP.

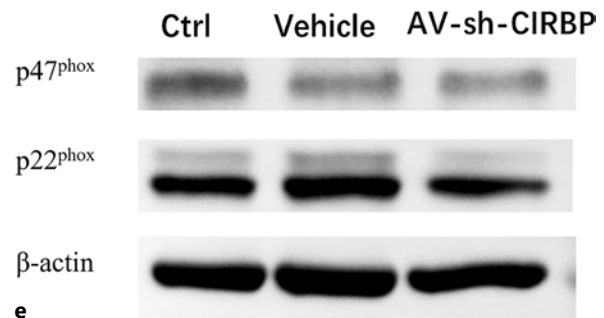
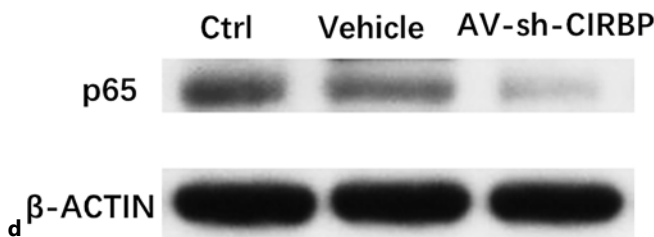
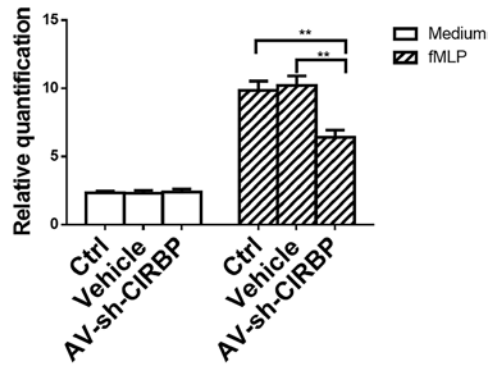
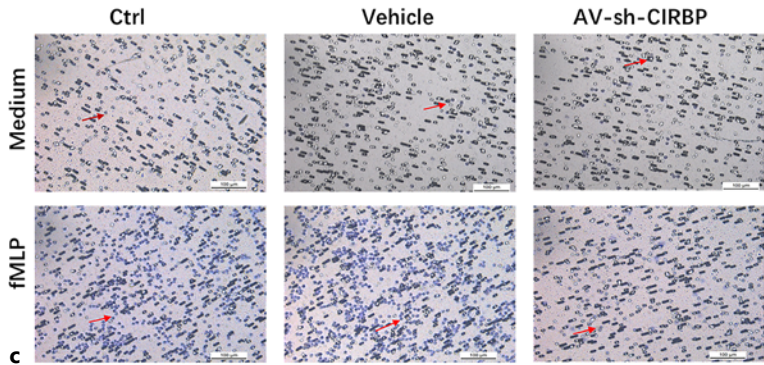
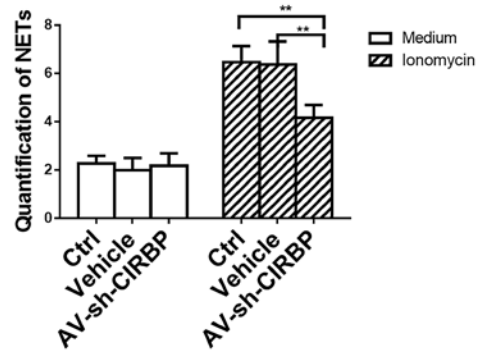
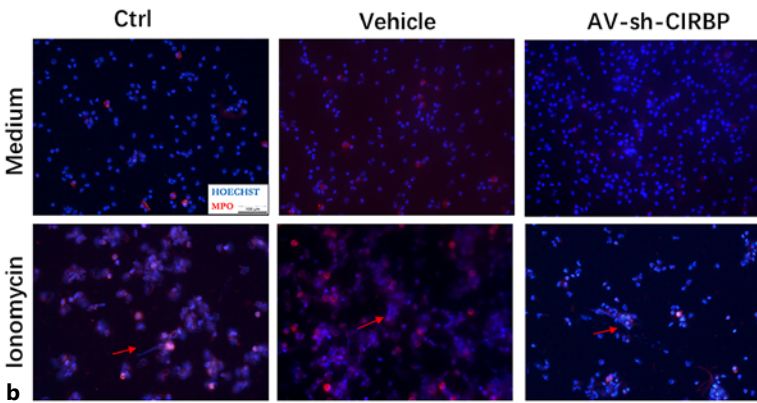
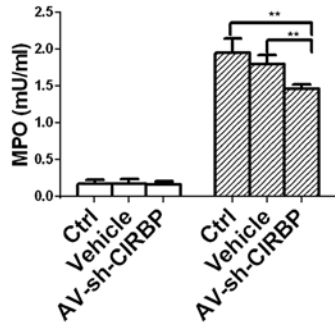
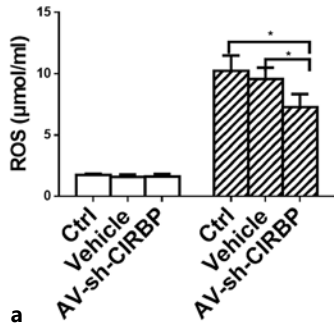
CIRBP is a member of the cold shock protein family induced by cold stress or hypoxia [46], and extracellular CIRBP has been proved to play a role as a damage-associated molecular pattern that accelerates systemic inflammation and even organ injury [44]. As a target of extracellular CIRBP, neutrophils could be activated through the TLR4-MyD88 pathway and release NETs consequently [47]. However, the immunoregulatory effects of intracellular CIRBP (iCIRBP) on neutrophils are still unknown. To explore the potential immunoregulatory role of iCIRBP in modulating neutrophils, we knocked down CIRBP expression in dHL-60 cells by transfection with AV-sh-CIRBP (online Suppl. Fig. 10b). Consequently,

Fig. 5. MCPIP-1 binds and degrades the mRNA of CIRBP. **a** Heatmap of differentially expressed genes ($|\text{fold change}| > 1.5$ or $< 2/3$ and p value < 0.01) between *Mcpip*^{Mye-tg} ($n = 3$) and WT ($n = 3$) neutrophils. **b** Correlation network of the differentially expressed genes between *Mcpip*^{Mye-tg} and WT neutrophils. **c** Expression of CIRBP was analyzed by qRT-PCR and normalized to GAPDH in dHL-60 cells when transfected in vitro with adenovirus vectors expressing MCPIP-1 (AV-MCPIP-1) or D141N mutant (AV-D141N) or with empty adenovirus vector (Ctrl). **d** RIP-seq analysis in dHL-60 cells was performed to show the enrichment of CIRBP mRNA in MCPIP and negative control protein. $*p < 0.05$.

the production of ROS and MPO, formation of NETs, and migratory capacity were markedly suppressed (Fig. 6a–c), and the expression of p65 was also decreased in AV-sh-CIRBP-transfected dHL-60 cells compared to controls (Fig. 6d). NADPH oxidase has been demonstrated to play a critical role in the downstream pathway of NF- κ B pathway [48]. To explore a potential way of iCIRBP to regulate the function of neutrophils, we analyzed the NADPH oxidase subunit p47^{phox} and the membrane-associated subunit p22^{phox} and found that knockdown of CIRBP expression markedly downregulated the phosphorylation of NADPH oxidase subunits in neutrophils (Fig. 6e). Taken together, these data indicate that MCPIP-1 binds and degrades the mRNA of CIRBP to suppress the protective functions of neutrophils and that iCIRBP functions as a potent effector to upregulate the activity of neutrophils via maintaining the NADPH oxidase activity.

MCPIP-1 Is Highly Expressed in Activated Neutrophils from Patients with Acute Infectious Diseases, Especially from Those with Liver Injury

Since our recent study has demonstrated that MCPIP-1 is highly expressed in neutrophils of patients with inflammatory bowel diseases [22], we then studied its expression in neutrophils in acute critical infectious diseases (e.g., CDE, severe acute pancreatitis, acute suppurative appendicitis, and CABP). Intriguingly, we found that expression of MCPIP-1 markedly increased in peripheral neutrophils from these patients compared to healthy donors (Fig. 7a, b; online Suppl. Table 1), particularly in severe acute pancreatitis patients with liver damage diagnosed by an increase of liver function test results and abnormal architectural changes by B-ultrasonography and CT images (Fig. 7c). Given that several inflammatory mediators are released to the circulation or targeted organs under inflammatory conditions and that neutrophils are activated by various microbiota-derived antigens (e.g., LPS, PGN, and flagellin) through TLR recognition, we further determined that the expression of MCPIP-1 at the protein level was relatively low in neutrophils of healthy donors at the steady state but highly increased under stimulation with PGN, FSL, LPS, and flagellin, respectively (Fig. 7d, e). However, Pam3CSK4 appeared not to affect expression of MCPIP-1 (Fig. 7 d, e). Collectively, the results suggest that expression of MCPIP-1 is markedly increased in neutrophils of acute inflammatory diseases, especially those with liver injury, and induced by several inflammatory mediators. MCPIP-1 may be a potential target for restraining the progress of acute inflammatory diseases, especially bacterial peritonitis and liver damage.



(For legend see next page.)

Discussion

In this study, we investigated the roles of MCPIP-1 in regulating neutrophils and found that MCPIP-1 markedly restrained the ROS/MPO production and the formation of NETs and inhibited the migration of neutrophils. MCPIP-1-mediated immunomodulation of neutrophils exacerbated *S. typhimurium*-induced acute peritonitis and associated liver injury. Importantly, MCPIP-1 was illustrated to bind and degrade the mRNA of CIRBP and suppress the activity of neutrophils. Moreover, we found that expression of MCPIP-1 was increased in peripheral neutrophils from patients with ABP or bacterial pneumonia compared with healthy donors and that expression of MCPIP-1 was elevated when neutrophils were activated. Therefore, our results indicate that MCPIP-1-mediated immunosuppression of neutrophils plays an important role in regulating the functional alterations of neutrophils, particularly neutrophil homeostasis during ABP and liver injury.

Previous studies have shown that MCPIP-1 is increased under inflammatory conditions, which is dramatically induced when the NF- κ B pathway is activated and subsequently inhibits the process of NF- κ B pathway [13]. Moreover, MCPIP-1 is also involved in suppressing the noninfectious inflammation, such as LPS-induced sepsis and autoimmune diseases [20, 21, 49]. However, previous studies pointed out that MCPIP-1 deficiency in CD4⁺ T cell or pulmonary epithelial cells enhances the resistance to pathogen invasion by recruiting more immune cells, particularly neutrophils, into the site of infection in vitro [45, 50, 51]. It could be sup-

Fig. 6. MCPIP-1 downregulates the activity of neutrophils via degrading mRNA of CIRBP. The dHL-60 cells were transfected with AV-sh-CIRBP or empty adenovirus vector (vehicle) or cultured in a medium alone (ctrl). These cells were then stimulated with PMA (100 ng/mL) or ionomycin (4 μ g/mL) for 3 h. **a** Expression of ROS and MPO was measured. **b** Representative immunofluorescent images for detecting NETs (blue, Hoechst 33342; red, MPO) were shown. Scale bars, 100 μ m. The quantification of NETs was calculated according to the formula as described in the Methods section. **c** Transwell assays were measured. Representative images of the lower chambers of Transwell plates. Scale bars, 100 μ m. The black arrows indicate neutrophils stained by crystal violet. The histograms represented the relative quantification of the migratory capacity of neutrophils by measuring the OD values of each well according to the Methods. **d** Expression of p65 in dHL-60 cells was analyzed by Western blotting under different conditions. **e** Expression of p47^{phox} and p22^{phox} in dHL-60 cells was analyzed by Western blotting under different conditions. * $p < 0.05$; ** $p < 0.01$; *** $p < 0.001$; **** $p < 0.0001$.

posed the distinct roles of MCPIP-1 in the induction of noninfectious inflammation and infectious disorders, respectively. In this study, we utilized a *S. typhimurium*-induced acute peritonitis model and found that MCPIP-1 restrained myeloid cells, especially neutrophils, to migrate into the circulation, the abdominal cavity, and the liver as one of the targeted organs of peritonitis and that the CFUs of *S. typhimurium*, as a signature of bacterial peritonitis, were remarkably elevated consequently. As a result, *Mcpip*^{Mye-tg} mice developed severe peritonitis and associated liver injury after intraperitoneal infection with *S. typhimurium*. In contrast, bacterial peritonitis and associated liver injury could be alleviated in *Mcpip* ^{Δ Mye} mice. These results indicate that MCPIP-1 downregulates the protective functions of neutrophils in ABP and liver injury.

In the context of the invasion by exogenous pathogens, the neutrophils release ROS or MPO in the oxidative burst which could be mediated by the NF- κ B pathway [52]. Another way of neutrophil defense against pathogens is mediated by the formation of NETs, which are composed of cytosolic and granule proteins (e.g., MPO, NE, and CitH3) as well as DNA and released to trap the pathogens and prevent dissemination [11]. We observed that MCPIP-1 remarkably inhibited the production of ROS and MPO and the formation of NETs and prohibited the migration of neutrophils by Transwell analysis. Intriguingly, we also observed that the expression of CXCL-1, CXCL-2, and CXCL-5 was suppressed in the liver tissues of *Mcpip*^{Mye-tg} mice but increased in *Mcpip* ^{Δ Mye} mice, in agreement with our recent data showing that the response of neutrophils to chemokines is restrained by MCPIP-1 [22]. We also found that MCPIP-1 was unable to alter the phagocytosis of neutrophils, which is mediated by pattern recognition receptors. MCPIP-1 may not affect the activity of PRR-pathogen-associated molecular pattern interactions but functions via the NF- κ B pathway that plays a key role in ROS release and NET formation. Therefore, these findings indicate that MCPIP-1 fine-tunes the immune responses of neutrophils against pathogen infection without altering the ability of pathogen recognition and that MCPIP-1 may play a detrimental role in antimicrobial progress.

In contrast to the compromised MCPIP-1-mediated migratory capacity of neutrophils in the liver tissues, excessive pathogenic FasL⁺ IFN- γ ⁺ TNF- α ⁺ NK cells were found to be highly infiltrated in the liver. Mechanistically, a CX3CL1-CX3CR1 axis, a key pathway involved in recruiting NK cells, was observed to be elevated in the liver, which thus contributes to excessive NK cell infiltration

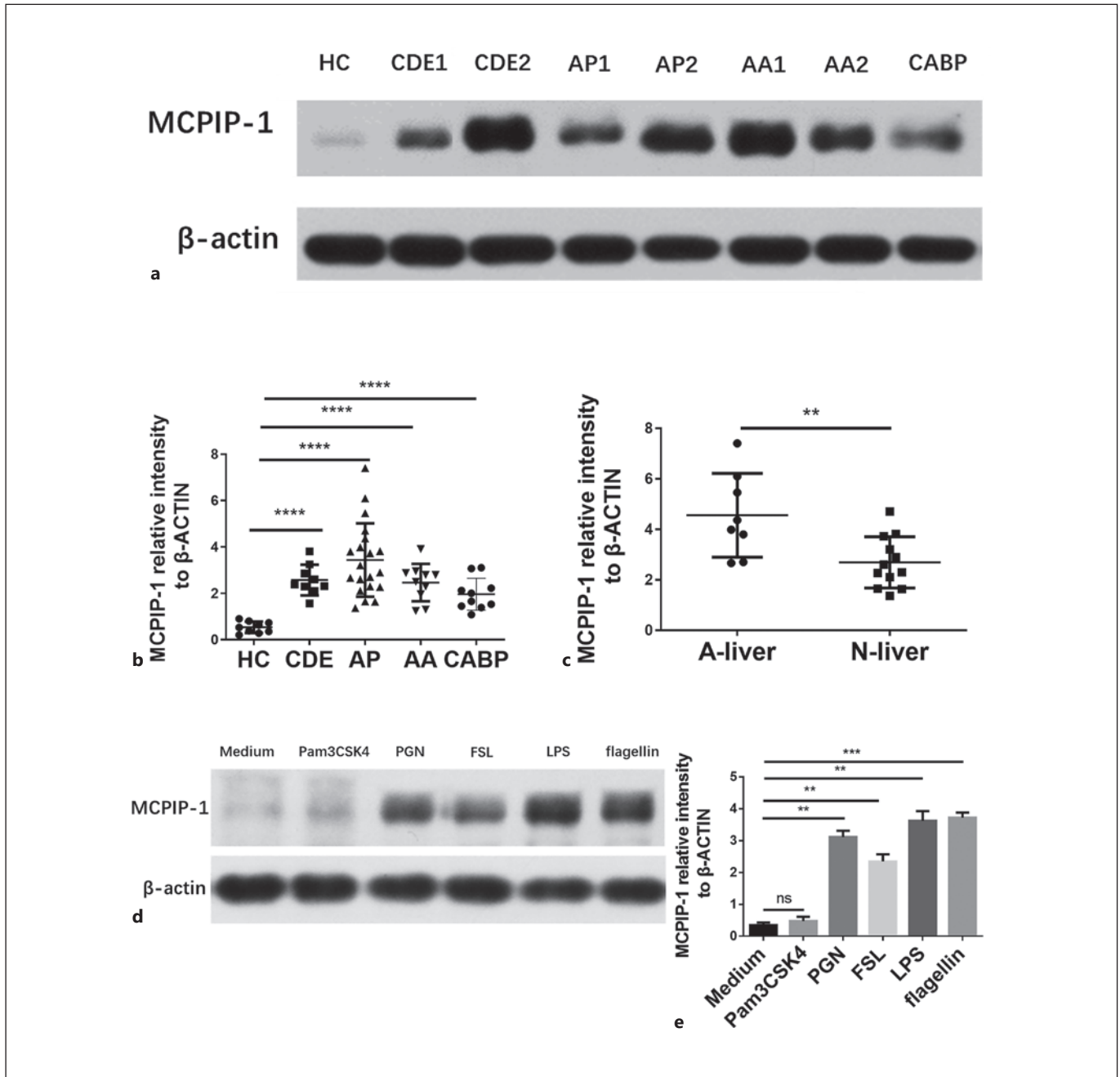


Fig. 7. MCPIP-1 is highly expressed in neutrophils of acute infectious diseases. Peripheral neutrophils were obtained from patients with active Crohn's disease with peritoneal exudation (CDE, $n = 10$), patients with severe acute pancreatitis (AP, $n = 20$), patients with acute appendicitis (AA, $n = 10$), patients with community-acquired bacterial pneumonia (CABP, $n = 10$), and healthy donors ($n = 10$). **a, b** Protein levels of MCPIP were determined by Western blotting (**a**) and quantified in gray value (**b**). **c** Expression of MCPIP in neutrophils of patients with acute severe pancreatitis who had abnormal liver function tests (A-liver, $n = 8$) and normal liver function tests (N-liver, $n = 12$), respectively. **d, e** Neutrophils

from healthy controls ($n = 5$) were stimulated in vitro with Pam3CSK4 (1 $\mu\text{g}/\text{mL}$), FSL (100 ng/mL), LPS (100 ng/mL), flagellin (100 ng/mL), and PGN (1 $\mu\text{g}/\text{mL}$), respectively, and harvested 3 h after culture. The protein levels of MCPIP were determined by Western blotting (**d**) and quantified in gray value (**e**). * $p < 0.05$; ** $p < 0.01$; *** $p < 0.001$; **** $p < 0.0001$. ns, not significant; HC, healthy controls; CDE, active Crohn's disease patients with peritoneal exudation; AP, acute pancreatitis; AA, acute appendicitis; CABP, community-acquired bacterial pneumonia; A-liver, abnormal liver function tests; N-liver, normal liver function tests.

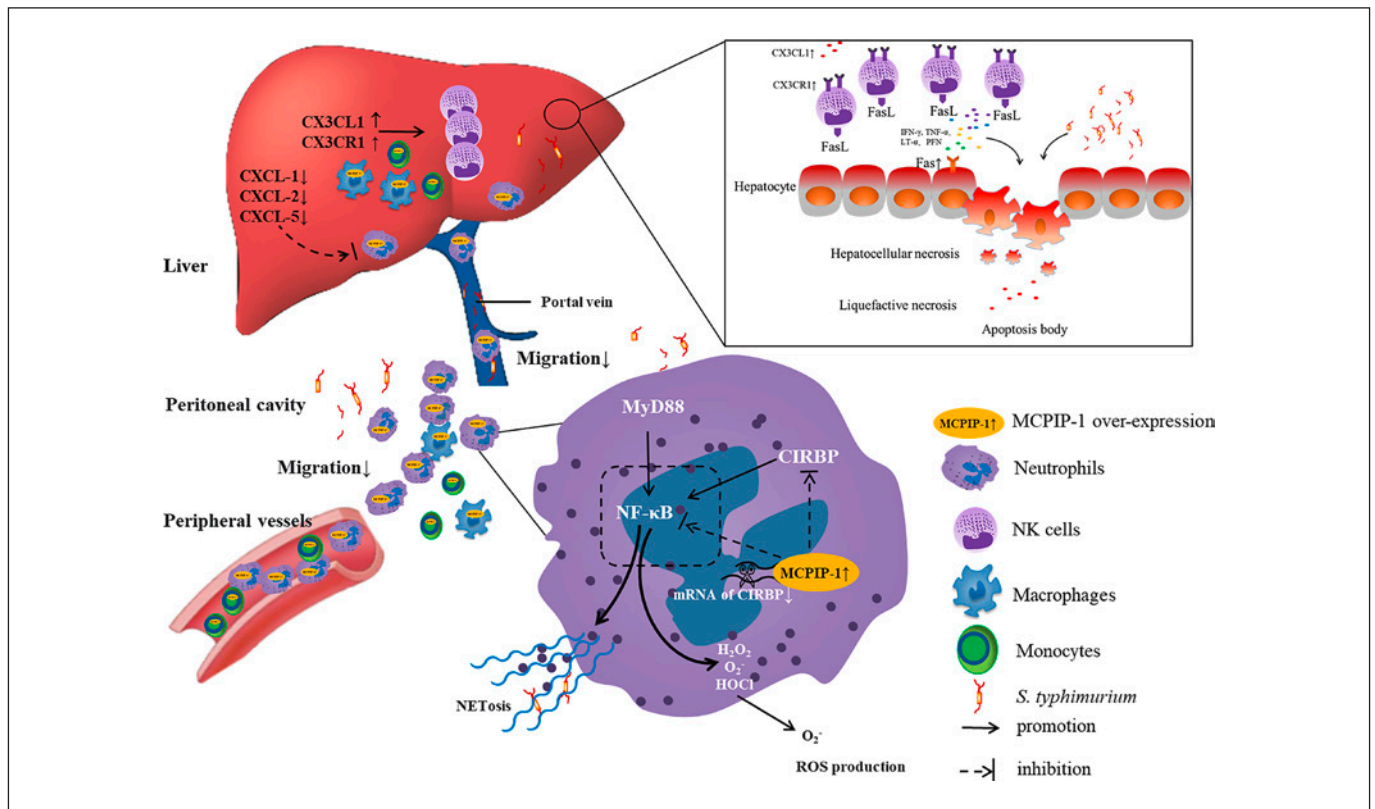


Fig. 8. Schematic representative of the role of MCPIP-1 in modulating neutrophil functions. MCPIP-1 not only suppresses the production of ROS and MPO, the formation of NETs, and the migratory capacity of neutrophils but also downregulates the recruitment of myeloid cells and pathogen clearance at the sites of inflammation. In the context of intraperitoneal infection with *S.*

typhimurium, MCPIP-1 inhibits the migration of myeloid cells from peripheral blood into the peritoneum and liver tissues, leading to severe bacterial peritonitis. Mechanically, MCPIP-1 binds and degrades the mRNA of CIRBP to suppress the protective function of neutrophils and exacerbate the bacteria-induced acute peritonitis and associated liver damage.

concomitantly. Therefore, our findings indicate that MCPIP-1-mediated immunosuppression of neutrophils fails to eliminate pathogens but induces excessive NK cell infiltration, leading to secondary liver injury accompanied by an increase of ALT and AST and the presence of the liquefactive necrosis.

Most importantly, we clarified that CIRBP functions as a critical immune effector in promoting the activities of neutrophils. As a member of RNA-binding proteins, CIRBP consists of an N-terminal RNA recognition motif and a C-terminal arginine-rich region structurally similar to stress-induced RNA-binding proteins in various species [53]. Unlike MCPIP-1 by degrading target mRNAs, CIRBP prevents the target mRNAs from deadenylation and maintains mRNA stability [54]. Increasing lines of evidence have shown the potential roles of CIRBP in the regulation of a variety of cellular stress responses, including cell proliferation, cell survival, and circadian clock

gene modulation [46], and illustrated that CIRBP enhances the NK-κB activity which is essential for the immune response in neutrophils [55]. In this study, we found that CIRBP deficiency led to suppressing the production of ROS and MPO, the formation of NETs, and the recruitment of neutrophils, as well as the NK-κB activity in dHL-60 cells. Moreover, CIRBP enables to promote the immune function of neutrophils by maintaining the activity of NADPH oxidase. Therefore, our data unequivocally pinpoint that iCIRBP plays a crucial role in regulating the activity of neutrophils.

Finally, we identified that expression of MCPIP-1 was elevated in peripheral neutrophils from the patients with acute critical abdominal infectious diseases (i.e., CDE, severe acute pancreatitis, and acute suppurative appendicitis) or CABP and that an increase of MCPIP-1 was closely related to target organ injury, particularly liver damage. Since neutrophils play an essential role in the progress of

acute abdominal infection and liver injury and could be activated in peripheral circulation or local infectious sites by a variety of inflammatory mediators involved in peritonitis [2], increased expression of MCPIP-1 in these activated neutrophils delicately maintains the homeostasis and could be considered as a potential target for monitoring the outcome of acute inflammatory diseases. Even more, it may function as a therapeutic target to maintain the homeostasis of neutrophils in the progress of acute infectious diseases.

In summary, our data reveal that MCPIP-1 plays a critical role in negatively modulating the protective functions of neutrophils in pathogen infection and liver injury, which constrains pathogen clearance by neutrophils in the context of ABP (Fig. 8) and that its overexpression may be vulnerable to anti-infectious processes. However, it should be noticed that neutrophils, even other immune cells, will be overactivated under inflammatory conditions without the control of MCPIP-1. Hence, it may serve as a “brake” in regulating the immune response and function as a promising candidate in innate immunity to clarify the way and maintain the homeostasis of neutrophils. These data shed some light on better understanding the MCPIP-1-mediated immunosuppression of neutrophils and provide a novel therapeutic avenue for infection-driven liver injury.

Acknowledgments

We are grateful to Drs. Jianli Niu and Pappachen Kolattukudy from the Burnett School of Biomedical Science for offering *Mcpip*^{Mye-tg} mice, the MCPIP-1-LoxP mice, and LysM-Cre mice. We express gratitude to Dr. Guangxun Meng from the Shanghai Institute of Pasteur, Chinese Academy of Sciences, for providing the strain of *S. typhimurium*.

References

- 1 Angus DC, Linde-Zwirble WT, Lidicker J, Clermont G, Carcillo J, Pinsky MR. Epidemiology of severe sepsis in the United States: analysis of incidence, outcome, and associated costs of care. *Crit Care Med*. 2001;29(7):1303–10.
- 2 Xiao Z, Wilson C, Robertson HL, Roberts DJ, Ball CG, Jenne CN, et al. Inflammatory mediators in intra-abdominal sepsis or injury: a scoping review. *Crit Care*. 2015;19:373.
- 3 Hotchkiss RS, Opal S. Immunotherapy for sepsis: a new approach against an ancient foe. *N Engl J Med*. 2010;363(1):87–9.
- 4 Strnad P, Tacke F, Koch A, Trautwein C. Liver: guardian, modifier and target of sepsis. *Nat Rev Gastroenterol Hepatol*. 2017;14(1):55–66.
- 5 Schnabl B, Brenner DA. Interactions between the intestinal microbiome and liver diseases. *Gastroenterology*. 2014;146(6):1513–24.
- 6 Jenne CN, Kubes P. Immune surveillance by the liver. *Nat Immunol*. 2013;14(10):996–1006.
- 7 Chen H, Wu X, Xu C, Lin J, Liu Z. Dichotomous roles of neutrophils in modulating pathogenic and repair processes of inflammatory bowel diseases. *Precis Clin Med*. 2021;4(4):246–57.
- 8 Kolaczowska E, Kubes P. Neutrophil recruitment and function in health and inflammation. *Nat Rev Immunol*. 2013;13(3):159–75.
- 9 Zygiel EM, Nolan EM. Transition metal sequestration by the host-defense protein calprotectin. *Annu Rev Biochem*. 2018;87:621–43.

Statement of Ethics

This study protocol was reviewed and approved by the Institutional Review Board for Clinical Research of Shanghai Tenth People's Hospital of Tongji University, approval number: SHSY-IEC-40.0/19-37/01). Animal study protocol was reviewed and approved by the Institutional Animal Care and Use Committee of the Tongji University, approval number: SHDSYY-2018-1966. Written informed consent was obtained from participants (or their parent/legal guardian/next of kin) to participate in the study.

Conflict of Interest Statement

The authors have declared that no conflict of interest exists.

Funding Sources

This work is supported by grants from the National Natural Science Foundation of China (91942312, 81630017).

Author Contributions

Zhanju Liu planned and supervised the experimental work and performed data analyses. Jian Lin, Zhanjun Lu, and Gengfeng Li performed all experiments. Huiying Lu, Cui Zhang, Sheng Gao, and Ruixin Zhu analyzed the data. Huili Wu and Zhanju Liu contributed to the clinical data and specimens. Hailiang Huang, Konrad Aden, Jianhua Wang, and Yingzi Cong analyzed and interpreted results. Jian Lin and Zhanju Liu wrote the manuscript. All the authors revised the manuscript and approved it for submission.

Data Availability Statement

All data generated or analyzed during this study are included in this article and its online supplementary material. Further inquiries can be directed to the corresponding author.

- 10 Dupré-Crochet S, Erard M, Nüße O. ROS production in phagocytes: why, when, and where? *J Leukoc Biol*. 2013;94(4):657–70.
- 11 Papayannopoulos V. Neutrophil extracellular traps in immunity and disease. *Nat Rev Immunol*. 2018;18(2):134–47.
- 12 Matute-Bello G, Frevet CW, Kajikawa O, Skerrett SJ, Goodman RB, Park DR, et al. Septic shock and acute lung injury in rabbits with peritonitis: failure of the neutrophil response to localized infection. *Am J Respir Crit Care Med*. 2001;163(1):234–43.
- 13 Liang J, Wang J, Azfer A, Song W, Tromp G, Kolattukudy PE, et al. A novel CCCH-zinc finger protein family regulates proinflammatory activation of macrophages. *J Biol Chem*. 2008;283(10):6337–46.
- 14 Matsushita K, Takeuchi O, Standley DM, Kumagai Y, Kawagoe T, Miyake T, et al. Zc3h12a is an RNase essential for controlling immune responses by regulating mRNA decay. *Nature*. 2009;458(7242):1185–90.
- 15 Liang J, Saad Y, Lei T, Wang J, Qi D, Yang Q, et al. MCP-induced protein 1 deubiquitinates TRAF proteins and negatively regulates JNK and NF-kappaB signaling. *J Exp Med*. 2010;207(13):2959–73.
- 16 Mizgalska D, Wegrzyn P, Murzyn K, Kasza A, Koj A, Jura J, et al. Interleukin-1-inducible MCP1P protein has structural and functional properties of RNase and participates in degradation of IL-1beta mRNA. *FEBS J*. 2009;276(24):7386–99.
- 17 Suzuki HI, Arase M, Matsuyama H, Choi YL, Ueno T, Mano H, et al. MCP1P1 ribonuclease antagonizes dicer and terminates microRNA biogenesis through precursor microRNA degradation. *Mol Cell*. 2011;44(3):424–36.
- 18 Uehata T, Iwasaki H, Vandenbon A, Matsushita K, Hernandez-Cuellar E, Kuniyoshi K, et al. Malt1-induced cleavage of regnase-1 in CD4(+) helper T cells regulates immune activation. *Cell*. 2013;153(5):1036–49.
- 19 Marona P, Gorka J, Mazurek Z, Wilk W, Rys J, Majka M, et al. MCP1P1 downregulation in clear cell renal cell carcinoma promotes vascularization and metastatic progression. *Cancer Res*. 2017;77(18):4905–20.
- 20 Huang S, Miao R, Zhou Z, Wang T, Liu J, Liu G, et al. MCP1P1 negatively regulates toll-like receptor 4 signaling and protects mice from LPS-induced septic shock. *Cell Signal*. 2013;25(5):1228–34.
- 21 Li Y, Huang X, Huang S, He H, Lei T, Saaoud F, et al. Central role of myeloid MCP1P1 in protecting against LPS-induced inflammation and lung injury. *Signal Transduct Target Ther*. 2017;2:17066.
- 22 Lin J, Li G, Xu C, Lu H, Zhang C, Pang Z, et al. Monocyte chemotactic protein 1-induced protein 1 is highly expressed in inflammatory bowel disease and negatively regulates neutrophil activities. *Mediators Inflamm*. 2020;2020:8812020.
- 23 Lehman HK, Segal BH. The role of neutrophils in host defense and disease. *J Allergy Clin Immunol*. 2020;145(6):1535–44.
- 24 Kapoor N, Niu J, Saad Y, Kumar S, Sirakova T, Becerra E, et al. Transcription factors STAT6 and KLF4 implement macrophage polarization via the dual catalytic powers of MCP1P. *J Immunol*. 2015;194(12):6011–23.
- 25 Lu H, Lin J, Xu C, Sun M, Zuo K, Zhang X, et al. Cyclosporine modulates neutrophil functions via the SIRT6-HIF-1 α -glycolysis axis to alleviate severe ulcerative colitis. *Clin Transl Med*. 2021;11(2):e334.
- 26 Yadav S, Pathak S, Sarikhani M, Majumdar S, Ray S, Chandrasekar BS, et al. Nitric oxide synthase 2 enhances the survival of mice during *Salmonella typhimurium* infection-induced sepsis by increasing reactive oxygen species, inflammatory cytokines and recruitment of neutrophils to the peritoneal cavity. *Radic Biol Med*. 2018;116:73–87.
- 27 Lin R, Wu W, Chen H, Gao H, Wu X, Li G, et al. GPR65 promotes intestinal mucosal Th1 and Th17 cell differentiation and gut inflammation through downregulating NUA2. *Clin Transl Med*. 2022;12(3):e771.
- 28 Lin R, Ma C, Fang L, Xu C, Zhang C, Wu X, et al. TOB1 blocks intestinal mucosal inflammation through inducing ID2-mediated suppression of Th1/Th17 cell immune responses in IBD. *Cell Mol Gastroenterol Hepatol*. 2022;1313(4):1201–21.
- 29 Manda-Handzlik A, Bystrzycka W, Wachowska M, Sieczkowska S, Stelmaszczyk-Emmel A, Demkow U, et al. The influence of agents differentiating HL-60 cells toward granulocyte-like cells on their ability to release neutrophil extracellular traps. *Immunol Cell Biol*. 2018;96(4):413–25.
- 30 Li G, Lin J, Zhang C, Gao H, Lu H, Gao X, et al. Microbiota metabolite butyrate constrains neutrophil functions and ameliorates mucosal inflammation in inflammatory bowel disease. *Gut Microbes*. 2021;13(1):e1968257.
- 31 Tsai MC, Manor O, Wan Y, Mosammaparast N, Wang JK, Lan F, et al. Long noncoding RNA as modular scaffold of histone modification complexes. *Science*. 2010;329(5992):689–93.
- 32 Dobosz E, Wadowska M, Kaminska M, Wilamowski M, Honarpisheh M, Bryzek D, et al. MCP1P-1 restricts inflammation via promoting apoptosis of neutrophils. *Front Immunol*. 2021;12:e627922.
- 33 Deng W, Yang Z, Yue H, Ou Y, Hu W, Sun P. Disulfiram suppresses NLRP3 inflammasome activation to treat peritoneal and gouty inflammation. *Free Radic Biol Med*. 2020;152:8–17.
- 34 Jorch SK, Surewaard BG, Hossain M, Peiseler M, Deppermann C, Deng J, et al. Peritoneal GATA6+ macrophages function as a portal for *Staphylococcus aureus* dissemination. *J Clin Invest*. 2019;129(11):4643–56.
- 35 Marques PE, Amaral SS, Pires DA, Nogueira LL, Soriani FM, Lima BHF, et al. Chemokines and mitochondrial products activate neutrophils to amplify organ injury during mouse acute liver failure. *J Hepatology*. 2012;56(5):1971–82.
- 36 Campbell SJ, Jiang Y, Davis AEM, Farrands R, Holbrook J, Leppert D, et al. Immunomodulatory effects of etanercept in a model of brain injury act through attenuation of the acute-phase response. *J Neurochem*. 2007;103(6):2245–55.
- 37 Chen Q, Wei H, Sun R, Zhang J, Tian Z. Therapeutic RNA silencing of Cys-X3-Cys chemokine ligand 1 gene prevents mice from adenovirus vector-induced acute liver injury. *Hepatology*. 2008;47(2):648–58.
- 38 Beraza N, Malato Y, Sander LE, Al-Masaoudi M, Freimuth J, Riethmacher D, et al. Hepatocyte-specific NEMO deletion promotes NK/NKT cell- and TRAIL-dependent liver damage. *J Exp Med*. 2009;206(8):1727–37.
- 39 Rehermann B. Pathogenesis of chronic viral hepatitis: differential roles of T cells and NK cells. *Nat Med*. 2013;19(7):859–68.
- 40 Jeong WI, Park O, Suh YG, Byun JS, Park SY, Choi E, et al. Suppression of innate immunity (natural killer cell/interferon- γ) in the advanced stages of liver fibrosis in mice. *Hepatology*. 2011;53(4):1342–51.
- 41 Lian RH, Kumar V. Murine natural killer cell progenitors and their requirements for development. *Semin Immunol*. 2002;14(6):453–60.
- 42 Tian Z, Chen Y, Gao B. Natural killer cells in liver disease. *Hepatology*. 2013;57(4):1654–62.
- 43 Geng J, Wang X, Wei H, Sun R, Tian Z. Efficient attenuation of NK cell-mediated liver injury through genetically manipulating multiple immunogenes by using a liver-directed vector. *J Immunol*. 2013;190(9):4821–9.
- 44 Qiang X, Yang WL, Wu R, Zhou M, Jacob A, Dong W, et al. Cold-inducible RNA-binding protein (CIRP) triggers inflammatory responses in hemorrhagic shock and sepsis. *Nat Med*. 2013;19(11):1489–95.
- 45 Mino T, Murakawa Y, Fukao A, Vandenbon A, Wessels HH, Ori D, et al. Regnase-1 and roquin regulate a common element in inflammatory mRNAs by spatiotemporally distinct mechanisms. *Cell*. 2015;161(5):1058–73.
- 46 Nishiyama H, Danno S, Kaneko Y, Itoh K, Yokoi H, Fukumoto M, et al. Decreased expression of cold-inducible RNA-binding protein (CIRP) in male germ cells at elevated temperature. *Am J Pathol*. 1998;152(1):289–96.
- 47 Chen K, Murao A, Arif A, Takizawa S, Jin H, Jiang J, et al. Inhibition of efferocytosis by extracellular cirp-induced neutrophil extracellular traps. *J Immunol*. 2021;206(4):797–806.

- 48 Han W, Li H, Cai J, Gleaves LA, Polosukhin VV, Segal BH, et al. NADPH oxidase limits lipopolysaccharide-induced lung inflammation and injury in mice through reduction-oxidation regulation of NF- κ B activity. *J Immunol*. 2013;190(9):4786–94.
- 49 Dobosz E, Lorenz G, Ribeiro A, Würf V, Wadowska M, Kotlinowski J, et al. Murine myeloid cell MCP1P1 suppresses autoimmunity by regulating B-cell expansion and differentiation. *Dis Model Mech*. 2021;14(3):dmm047589.
- 50 Garg AV, Amatya N, Chen K, Cruz JA, Grover P, Whibley N, et al. MCP1P1 endoribonuclease activity negatively regulates interleukin-17-mediated signaling and inflammation. *Immunity*. 2015;43(3):475–87.
- 51 Nakatsuka Y, Vandenbon A, Mino T, Yoshinaga M, Uehata T, Cui X, et al. Pulmonary Regnase-1 orchestrates the interplay of epithelium and adaptive immune systems to protect against pneumonia. *Mucosal Immunol*. 2018;11(4):1203–18.
- 52 Dahlgren C, Karlsson A, Bylund J. Intracellular neutrophil oxidants: from laboratory curiosity to clinical reality. *J Immunol*. 2019; 202(11):3127–34.
- 53 Nishiyama H, Itoh K, Kaneko Y, Kishishita M, Yoshida O, Fujita J. A glycine-rich RNA-binding protein mediating cold-inducible suppression of mammalian cell growth. *J Cell Biol*. 1997;137(4):899–908.
- 54 Xia Z, Zheng X, Zheng H, Liu X, Yang Z, Wang X. Cold-inducible RNA-binding protein (CIRP) regulates target mRNA stabilization in the mouse testis. *FEBS Lett*. 2012; 586(19):3299–308.
- 55 Lujan DA, Ochoa JL, Hartley RS. Cold-inducible RNA binding protein in cancer and inflammation. *Wiley Interdiscip Rev RNA*. 2018;9(2):e1462.